



LUND  
UNIVERSITY



HOST UNIVERSITY: Lund University

FACULTY: Faculty of Engineering

DEPARTMENT: Division of Fire Safety Engineering

Academic year 2017-2018

## **Identification and characterization of design fires to be used in performance-based fire design of CERN facilities**

Darko Perović

Supervisors:

Patrick Van Hees, Lund University

Oriol Rios Rubiras, CERN

Saverio La Mendola, CERN

Master thesis submitted in the Erasmus Mundus Study Program

**International Master of Science in Fire Safety Engineering**

# Disclaimer

This thesis is submitted in partial fulfilment of the requirements for the degree of *The International Master of Science in Fire Safety Engineering (IMFSE)*. This thesis has never been submitted for any degree or examination to any other University/programme. The author(s) declare(s) that this thesis is original work except where stated. This declaration constitutes an assertion that full and accurate references and citations have been included for all material, directly included and indirectly contributing to the thesis. The author(s) gives (give) permission to make this master thesis available for consultation and to copy parts of this master thesis for personal use. In the case of any other use, the limitations of the copyright have to be respected, in particular with regard to the obligation to state expressly the source when quoting results from this master thesis. The thesis supervisor must be informed when data or results are used.

*Read and approved*



Darko Perović

April 30<sup>th</sup>, 2018

# Abstract

CERN operates the most complex particle accelerator facility built until today. As such, it consists of thousands of custom-made components spread both in upper ground facilities and in underground tunnels and caverns. Several different hazards, including fire, are present in these facilities and need to be reduced to a tolerable level; in particular, fire safety often requires the application of a scientific and engineering approach. As it would be impossible addressing each tiny component individually, envelope conservative solutions have to be developed in order to save both financial and time resources.

This thesis is aimed at characterizing and better understanding of the potential fire behaviour of most common combustible items present in CERN's facilities. After a detailed literature review of fires in electronic cabinets, an Excel calculator for obtaining a design fire in any number of cabinets/racks is developed. As literature for small vehicles in fires is scarce, suggestions on how to address the fires in vehicles used at CERN are given.

Second part of the thesis is dedicated to exploring testing techniques suitable for CERN's needs with the goal of characterizing smoke produced by the most common cables and insulating oils used at CERN. Particle size distribution is obtained by using DMS500 fast particle analyser (Cambusiton), coupled with cone calorimeter (FTT). Data obtained on smoke particles will in future be used to validate and further improve FDS (Fire Dynamics Simulator) code in terms of addressing this issue. CERN is particularly interested in knowing the smoke particle size distribution that can be expected, as radioactive particles could be carried around, and endanger the whole facility and the surrounding environment.

# Rezime

CERN upravlja najkompleksnijim postrojenjem akceleratora čestica izgrađenim do današnjeg dana. Kao takvo, sastoji se od hiljada komponenti napravljenih za specifičnu upotrebu, rasprostranjenih kako u nadzemnim objektima, tako i u podzemnim tunelima i prostorijama. Opasnosti, uključujući i one od požara, su brojne i nezanemarljive, te zaslužuju ozbiljnu pažnju kao i naučni i inženjerski pristup u rešavanju. Budući da bi bilo nemoguće baviti se svakom sitnom komponentom pojedinačno, sveobuhvatna, konzervativna rešenja moraju biti pronađena sa ciljem uštede kako finansijskih tako i vremenskih resursa.

Ova teza je usmerena ka karakterizaciji i boljem razumevanju potencijalnog ponašanja prilikom požara najprisutnijih predmeta korišćenih u CERNu. Nakon detaljne analize literature koja se bavila požarima u električnim kabinetima, napravljen je Excel kalkulator za dobijanje projektovanog požara u bilo kom broju električnih kabinetova / rafova. Pošto je literatura o požarima u malim vozilima oskudna, date su sugestije o tome kako da se pristupi požarima u vozilima prisutnim u CERNu.

Drugi deo teze je posvećen istraživanju eksperimentalnih tehnika usklađenim sa potrebama CERNa, sa ciljem karakterizacije dima proizvedenog pri gorenju najprisutnijih kablova i izolacionih ulja korišćenih u CERNu. Distribucija čestica dima po veličini je dobijena koristeći DMS500 brzi čestični analizator (Cambustion), uparen sa konusnim kalorimetrom (FTT). Podaci o česticama dobijeni u ovim eksperimentima će u budućnosti biti korišćeni da se validira i dalje razvije FDS (Fire Dynamics Simulator – simulator dinamike vatre) kod za ovaj domen. CERN je posebno zainteresovan da sazna očekivanu raspodelu veličina čestica, jer su čestice u mogućnosti da dalje prenose radijaciju i time ugroze kako samo postrojenje, tako i okruženje.

# TABLE OF CONTENTS

---

List of figures.....	6
List of tables .....	8
List of symbols.....	8
1    Introduction .....	9
1.1    Overall objective .....	10
1.2    Thesis structure .....	10
1.3    Limitations.....	11
1.4    Literature review .....	11
1.4.1    Electrical Cabinets .....	12
Conclusions for electrical cabinets literature review: .....	14
1.4.2    Vehicle fires.....	15
Conclusions for vehicle fires literature review .....	15
1.4.3    Particle size analysis .....	16
Conclusions for particle size analysis literature review .....	18
2    Methodology.....	19
2.1    Electrical Cabinets and Racks .....	19
2.1.1    Theory – Design fires.....	19
2.1.2    Design fires for electrical cabinets and racks .....	20
2.1.3    Comparison of values used in Excel calculator with modelled values in France / Finland	27
Note for confined environment case .....	28
2.2    Vehicle fires.....	29
2.3    Particulate Matter analysis .....	32
2.3.1    Experimental setup.....	32
2.3.2    Samples preparation.....	35
2.3.3    Conducting the experiments .....	38
3    Results and Discussion.....	41
3.1    Concentration graphs – Shell Diala and Blue Cables (C01) .....	41
3.2    Major graphs for all specimens.....	44
3.3    3D plots .....	54
3.4    Summary of experimental results .....	56

4	Conclusions and future work.....	57
4.1	Conclusions .....	57
4.2	Future work .....	58
5	Acknowledgments.....	59
6	References .....	60
7	Appendices .....	63
7.1	Appendix A – concentration graphs .....	63
7.2	Appendix B – 3D plots.....	66
7.3	Appendix C – CO and CO <sub>2</sub> yields.....	68
7.4	Appendix D – Total concentration graphs- all 3 tests.....	69
7.5	Appendix E – HRR graphs – all 3 tests.....	70
7.6	Appendix F – Smoke Production Rate vs Concentrations - cables .....	72
7.7	Appendix G – excel calculator explanation.....	74

## LIST OF FIGURES

---

Figure 1 - Soot size distribution and number in the smoke of HFFR cables (MLC/FTIR/ELPI – 25, 35, 50, 75 kW/m <sup>2</sup> ) [18].....	16
Figure 2 - Open/closed cabinets + racks in a row – picture from one of CERN facilities.....	21
Figure 3 - 2x10 electrical cabinets – picture from one of CERN facilities .....	21
Figure 4 - HRR for open cabinet or rack.....	22
Figure 5 - HRR for closed cabinet .....	23
Figure 6 - Time (min) for fire spread to adjacent cabinets.....	25
Figure 7 - 2*10 Open cabinets (or racks) - worst case scenario .....	25
Figure 8 - 2*10 Closed cabinets - extreme but most probable scenario .....	26
Figure 9 - HRR for 8 closed and 4 open cabinets (distribution 2C, 2O, 4C, 2O, 2C) .....	26
Figure 10 - Fire development in forklift fire, extracted from [17] .....	30
Figure 11 - Electrical tractor used in CERN.....	30
Figure 12 – Heated sample line connection to cone calorimeter	
Figure 13 - Connection to the main control unit	33
Figure 14 - Classification section - extracted from DMS500 manual [32] .....	34
Figure 15 - Cable types - C01, C02 and C04.....	35
Figure 16 – Components of the specimen holder .....	36
Figure 17 – C01 in sample holder – ready for the test	
Figure 18 – C02 in sample holder – ready for the test	37
Figure 19 – Sample holder	
Figure 20 – Oil placed in the holder .....	38
Figure 21 – Blue Cables (C01) at the start of burning after the test	
Figure 22 – Blue cables (C01)	40
Figure 23 - Shell Diala oil, burning process .....	40
Figure 24 – 1st and 2nd mode concentrations .....	42
Figure 25 - total particle concentrations over time .....	42
Figure 26 - average particle concentration vs size .....	42
Figure 27 - average particle concentration - all runs .....	42
Figure 28 - Density correction for diesel engine exhaust.....	42
Figure 29 - Mass concentration .....	42
Figure 30 - 1st and 2nd mode concentrations .....	43
Figure 31 – Total particle concentrations over time .....	43
Figure 32 – average particle concentration vs size .....	43
Figure 33 - average particle concentration - all runs .....	43
Figure 34 - Density correction for diesel engine exhaust.....	43
Figure 35 - Mass concentration .....	43
Figure 36 - Concentration in all 3 tests .....	44
Figure 37 - HRR for all 3 tests – Midel oil.....	45
Figure 38 - HRR for all tests - Blue Cables (C01).....	46
Figure 39 - 1st and 2nd mode conc. – brown cables (C04).....	46
Figure 40 - Bimodal distribution - brown cables (C04).....	46
Figure 41 - Total concentration for all 3 tests - black cables (C02) .....	47

Figure 42 - Total concentrations - Blue cables (C01).....	48
Figure 43 - HRR & Total concentration - Midel .....	48
Figure 44 - HRR & Total concentration - Shell Dlala .....	49
Figure 45 - HRR & Total concentration - Blue Cables (C01).....	49
Figure 46 - HRR & Total concentration - Black Cables (C02) .....	50
Figure 47 - HRR & Total concentration - Brown Cables (C04).....	51
Figure 48 - Heat Release Rate vs Effective Heat of Combustion - Black cables (C02) .....	51
Figure 49 - Mass loss rate vs total concentration - Black cables.....	52
Figure 50 - Smoke production rate vs 2nd mode concentration - Black cables .....	53
Figure 51 - Smoke production rate vs 1st mode concentration - Black cables .....	53
Figure 52 - Concentration vs Mobility Diameter vs Time - Blue Cables (C01) – average from all 3 tests.....	54
Figure 53 - Concentration vs Mobility Diameter vs Time - Shell Diala – average from all 3 tests .....	55
Figure 54 - 1st and 2nd mode concentrations .....	63
Figure 55 - total particle concentrations over time .....	63
Figure 56 - average particle concentration vs size .....	63
Figure 57 - average particle concentration - all runs .....	63
Figure 58 - Density correction for diesel engine exhaust.....	63
Figure 59 - Mass concentration .....	63
Figure 60 - 1st and 2nd mode concentrations.....	64
Figure 61 - total particle concentrations over time .....	64
Figure 62 - average particle concentration vs size .....	64
Figure 63 - average particle concentration - all runs .....	64
Figure 64 - Density correction for diesel engine exhaust.....	64
Figure 65 - Mass concentration .....	64
Figure 66 - 1st and 2nd mode concentrations .....	65
Figure 67 - total particle concentrations over time .....	65
Figure 68 - average particle concentration vs size .....	65
Figure 69 - average particle concentration - all runs .....	65
Figure 70 - Density correction for diesel engine exhaust.....	65
Figure 71 - Mass concentration .....	65
Figure 72 - Concentration vs Mobility Diameter vs Time – black cables – average from all 3 tests.....	66
Figure 73 - Concentration vs Mobility Diameter vs Time – brown cables – average from all 3 tests.....	67
Figure 74 - Concentration vs Mobility Diameter vs Time – Midel oil – average from all 3 tests	67
Figure 75 - Total concentration - All 3 tests -Shell Diala .....	69
Figure 76 - Total concentration - All 3 tests - Brown cables (C04) .....	69
Figure 77 - HRR graphs - all 3 tests - Shell Diala oil .....	70
Figure 78 - HRR graphs - all 3 tests - Black Cables C02.....	70
Figure 79 - HRR graphs - all 3 tests - Brown Cables C04 .....	71
Figure 80 - 2nd mode conc. vs SPR - Blue Cables (C01).....	72

Figure 81 - 1st mode conc vs SPR - Blue Cables (C01) .....	72
Figure 82 - 2nd mode conc vs SPR - Brown cables (C04).....	73
Figure 83 - 1st mode conc vs SPR - Brown Cables (C04).....	73
Figure 84 - Excel calculator for electrical cabinets - main input/output sheet .....	74

## LIST OF TABLES

---

Table 1- Peak HRR values for various inlet/outlet ratios.....	28
Table 2 - Cables specifications .....	35
Table 3 - Times needed for conducting one full test.....	39
Table 4 – Shell diala – concentration graphs.....	42
Table 5 - Blue cables (C01) - concentration graphs.....	43
Table 6 - Summary of experimental results .....	56
Table 7- Concentration graphs - Midel oil .....	63
Table 8 - Concentration graphs - Black cables.....	64
Table 9 - Concentration graphs – brown cables .....	65
Table 10 - CO and CO <sub>2</sub> yields - all specimens .....	68

## LIST OF SYMBOLS

---

$A_i$ [m <sup>2</sup> ] – inlet opening area (Also marked as $S_{in}$ in IRSN equation (3))
$A_e$ [m <sup>2</sup> ] - outlet opening area (Also marked as $S_{out}$ in IRSN equation (3))
$g$ [m/s <sup>2</sup> ] – gravitational acceleration
$H$ [m] - the vertical distance between the inlet and the outlet openings;
$q^*$ [kg/s] - flow rate of air inside the box
$\dot{Q}$ [kW] – heat release rate
$S_{cab}$ [m <sup>2</sup> ] – is the cross sectional area of a cabinet
$T_\infty$ [K] – ambient temperature
$T_f$ [K] – flame temperature
$k_{in}$ and $k_{out}$ are pressure loss coefficients at inlet and outlet
$\Delta H_c$ [MJ/kg] – effective heat of combustion
$\rho_\infty$ [kg/m <sup>3</sup> ]- density of ambient air
$\chi$ [-] – combustion efficiency

# 1 INTRODUCTION

---

CERN (French "Conseil Européen pour la Recherche Nucléaire"), or European Organization for Nuclear Research, is the largest particle physics laboratory in the world. As such, it employs thousands of scientists and engineers from all around the globe working on cutting edge problems both from scientific (physicist) side, which is the main purpose of CERN, but also from the engineering side.

As CERN consists of numerous buildings and underground areas having tens of kilometres of tunnels and other complex constructions, the whole facility represents a great challenge from any standpoint. Having kilometres of wiring, thousands of electrical components and a huge number of various combustible materials present in facilities (electrical cabinets, klystrons, detectors, vehicles, cable trays, racks etc.) – fire safety obviously represents a concern that should be paid special attention to. The organization is fully aware of the fire risk and is taking the appropriate measures to reduce it as much as possible – having this thesis project being a part of that goal.

Since CERN is such a unique facility, using prescriptive based fire design for research infrastructures is not always possible nor recommendable. Therefore, as the thesis title says – performance-based fire design is needed.

In comparison to specification-based prescriptive design, performance-based design has three main advantages:

1. It allows the designer to address the unique features and uses of a building. [1]
2. It allows a better understanding of how a building would perform in the event of a fire. [1]
3. It ensures striking a real balance between safety level and safety measures accounting for interests of all stakeholders (cost, time, quality, etc.)

In 2016. Frida Olin and Erik Isaksson conducted a master thesis at Lund University under the title “Comparative study of risk analysis methods from a fire safety perspective - Case study of new underground facilities at CERN” [2]. Although the focus of their report was on risk analysis methods, they also proposed some design fires for electrical cabinets and cable trays. Those design fires were calculated with simple  $\alpha \cdot t^2$  correlations. In addition, simple calculations regarding fire propagating among the electrical cabinets, and from cabinets to cable trays, were performed.

As CERN is such a large research facility, more detailed studies and more precise calculations need to be performed in order to obtain a better assessment of the fire risk.

Long term objective of CERN is to develop a catalogue, containing detailed descriptions of combustible items present at CERN with their single and combined design fires, and the modes of fire propagation and other relevant characteristics (CO and CO<sub>2</sub> yields, smoke particle size distributions etc.). This thesis, thus, aims at contributing to this catalogue

## **1.1 OVERALL OBJECTIVE**

The first objective of this thesis is to assess the fire hazard imposed by electrical cabinets, racks and vehicles used at CERN, and to address them with appropriate design fires. Second objective is to characterize fires in vehicles present in CERN. Third and major objective is to characterize smoke particles caused by fires in most common cables and insulating oils used at CERN.

Deeper insight into the smoke characterization of the most commonly used cables in tunnels and of the most commonly used oils in klystrons will be obtained by conducting experiments.

To reach this objective three main goals have to be fulfilled:

1. Exploring all the existing research papers done on electrical cabinet fires. Finding the most appropriate cases to be compared with the CERN electrical cabinets. Gathering the specifications and pictures of the most common cabinets present in CERN. Developing an Excel calculator giving the expected design fires for any number and distribution of electric cabinets.
2. Do a literature review on vehicle fires and propose an appropriate way of addressing this hazard.
3. Conduct small scale experiments on oils and cables using cone calorimeter coupled with particle analyser in order to characterize the smoke.

## **1.2 THESIS STRUCTURE**

For the successful completion of this thesis, a thorough literature review on electrical cabinet fires, vehicle fires and particulate matter analysis needed to be done. Also, a lot of knowledge was obtained from the literature review, and it was an important part of the thesis development. It is thus important acknowledging that “literature review” chapter is an essential part of this thesis and should be given special attention before reading the rest of the thesis.

As majority of thesis development related to cabinet fires was dedicated to theoretical background and methodology, while the results were summarized in only three graphs, for the sake of easier following, it was the authors decision not to separate the two, but to leave the results (graphs) in the methodology section. Same principle was applied for vehicle fires. Therefore, the only section of this thesis that was discussed in the results part was experimental part on particulate matter analysis.

### **1.3 LIMITATIONS**

The major limitation for this thesis were time resources, at the first place because of the deadline for submitting the thesis – the end of April. It was quite time consuming organizing the experiments, getting the help from other involved people, booking free times for the lab, conducting the experiments, which lead to finally short time remaining for analysis of the results.

Due to those circumstances, certain limitations applied:

1. Not all the materials desired could be tested (e.g. 3 types of cables instead of 5).
2. Tests could not be performed under all the various desired conditions – different irradiances, cables in two or three layers, more repetitions etc.
3. As not everything could be tested, extensive literature data had to be used, which already had their own limitations, so that introduced a new constraint into the preciseness of the work.

Nevertheless, assessing fire hazard can be done in other ways – analytically or computationally, which can sometimes be more reasonable. Part of this thesis is also assessing and offering other engineering ways for solving the problem.

### **1.4 LITERATURE REVIEW**

Literature review was conducted using the following scientific browsers and catalogues:

Edinburgh university library – DiscoverEd, Lund university library – Lovisa, Serbian scientific database – Kobson, Science Direct and Research Gate websites, and general Google Scholar/Google search.

Literature review was conducted by searching for all the papers containing key words relevant to the topic of this thesis (e.g. particle matter, smoke, impactors, vehicle fires, electrical cabinet fires, forklift fire, DMS500 etc.). On top of that, an attempt was made to research all the important references found in those papers.

To author's knowledge, vast majority (if not all) of the research papers relevant for this thesis were found, used and listed in the "References" section.

### 1.4.1 Electrical Cabinets

In [3], results of series of full scale cabinet fire tests are presented. The goal of the experiments was to examine: the potential for a cabinet fire to ignite; the rate of development of a fire in a cabinet; the resulting room environment produced by a fire and the potential for a fire to spread to other cabinets. In all experiments, cabinets had closed doors. The effects of the following variables on fire development were investigated:

- a) Different ignition sources, b) cabinet styles, c) cabinet ventilation, d) fuel types, amounts and configuration

In this setup fire could propagate only within the fire cabinet, not to adjacent ones. In this case double walls (a wall for each cabinet) were present, as well as the air gap in between. That doesn't have to be the case, thus no general conclusions for the propagation should be made. In this study, in the worst-case fire could cause melting of plastic in adjacent cabinet. Smoke obscured the view within minutes and that appeared to be the sole serious problem. It is emphasized how the results are configuration and test specific thus one should be cautious when giving general conclusions. It is shown how crucial the ignition source and in situ fuel type are – drastically higher HRRs for unqualified over qualified cables (qualified made to be fire resistant – passed IEEE-383 tests, unqualified did not pass). Also, even more important are the ventilation conditions. Cabinets with open doors give way bigger HRR values.

Mangs and Keski-Rahkonen [4],[5] - conducted series of full scale fire experiments on electronic cabinets. The cabinets were again closed, with only small inlet and outlet ventilation openings. The setup consisted of the main "fire cabinet", a mock-up cabinet attached to it for studying the response of an adjoining cabinet, and another cabinet placed 1m away from the fire cabinet for examining the effect of fire to the neighbouring cabinets. As these experiments were carried out under a large exhaust hood – these conditions are a good approximation for a cabinet fire in a free space, and they don't describe a situation in which a cabinet is burning in a small room. In "burning in a small room (or a tunnel)" case the hot gases accumulate below the ceiling radiating energy to the lower parts of the room. The burning conditions inside the primary burning cabinet are not influenced much by the hot layer in the room because the replacement air is taken from the opening located near the floor, where the oxygen-rich cold layer is, therefore the present experiments still give direct information about the inside of a cabinet on fire, which is our key interest. Thus, the present results can be used as input data for room fire calculations.

Due to thermal expansion, in each of the experiments, some door gaps occurred, modifying the ventilation conditions, resulting in higher HRRs and in flames emerging out of the cabinet. That's how the key role of the ventilation conditions in the cabinet when determining the rate of heat release was clearly shown again. A simplified cabinet flow model assuming small vents and thus unidirectional flow is presented resulting in a simple equation for max HRR depending only on the ventilation areas and vertical distance between them. The model was validated by the experiments. The resulting equation for peak HRR is given in the following equation:

$$\dot{Q} = 4.3 * \sqrt{\frac{H}{\frac{3.3}{A_e^2} + \frac{1}{A_i^2}}} MW \quad (1)$$

Unlike in [3], in this case ignition in the adjoining cabinet was observed. The wall of the adjoining cabinet was 0.5mm thick, with no air gap between the cabinets, and the cables were attached to the wall. Fire spreading across the corridor is unlikely as a direct heat transfer process. It becomes possible via the hot gas layer that accumulates in the upper part of the room when the fire has grown big enough or through molten plastic which could flow across the corridor. The importance of the tight bottom of the cabinet become also clear. Burning melt or dripping components could quickly spread the fire under a false floor in a cable spreading area.

In [6] and [7] Mangs repeated similar experiments as in [4] and [5], and adjusted the previously developed cabinet flow model, resulting in an improved equation for HRR (Eq. 2), resulting in better matching with the experiments. Again, fire spread to adjacent cabinet occurred in all experiments, and was not possible for the 1m away cabinet.

$$\dot{Q} = 7.4 * \chi * \sqrt{\frac{H}{\frac{2.3}{A_e^2} + \frac{1}{A_i^2}}} MW \quad (2)$$

IRSN [8], [9] and [10] conducted series of experiment on closed and open cabinets. Experiments were usually remarkably reproducible, opening the way to a phenomenological description of this type of fire. Experiments were performed in order to validate the model developed by Mangs and Keski-Rahkonen (MKR model). As vents were rather large in comparison to the cabinet cross section, the unidirectional flow assumption could not stand, thus the MKR model was improved. The new Bernoulli equation describing the pressure drop between the vent was proposed. It took into account larger openings, by using improved opening coefficients and it also took into account acceleration of the fluid due to its heating. An equation for steady state mass flow rate  $q^*$  (equation 3) was developed, which when multiplied with a constant value of  $\Delta H_{c,air} = 3.144 \text{ MJ kg}^{-1}$  resulted in equation for peak HRR (equation 4), that greatly matched the experiments. This value was said to be a constant valid over a large range of fuels at standard conditions of pressure and oxygen concentration. Furthermore, the fire was divided into five stages – incubation stage, fast spread stage, combustion outside the cabinet, steady stage and decay stage, and predictive model for all five stages was proposed.

$$q^* = \rho_\infty \sqrt{2gH} * \sqrt{\frac{1 - \left(\frac{T_\infty}{T_f}\right)}{\left(\frac{k_{in}}{S_{in}^2}\right) + \left(\frac{T_f}{T_\infty}\right) * \left(\frac{k_{out}}{S_{out}^2}\right) + \left[\left(\frac{T_f}{T_\infty}\right) - 1\right] * \left(\frac{1}{S_{cab}^2}\right)}} \quad (3)$$

$$\dot{Q} = q^* * \Delta H_{c,air} \quad (4)$$

As a part of this experimental campaign, tests on cabinets in confined environment (room) were performed for the first time. Results obtained will be further discussed in methodology section of this thesis.

Electric Power Research Institute (EPRI) and U.S. Nuclear Regulation Commission [11] made a summary of the state of the art in nuclear power plant fire safety in the US, including the analysis of all the fire experiments done up to the moment of publishing. The purpose of the document was to serve the needs of a fire risk analysis team by providing a structured framework for the overall analysis, as well as specific recommended practices to address key aspects of the analysis. They gave values for peak HRR for open and closed cabinets, obtained as a 98<sup>th</sup> percentile from the previous experiments. The results represent an envelope case for all the fire experiments done on electrical cabinets.

Calculations and comparisons between the HRR values presented in this literature review will be presented and further discussed in the methodology part.

### **Conclusions for electrical cabinets literature review:**

Literature on fires in electrical cabinets is existing, but to a limited extent. To author's knowledge, only four experimental campaigns on cabinet fires have been performed up to today. Making conclusions and using the models presented in the mentioned papers is seen as the only feasible and sufficiently precise way of dealing with cabinet fires in CERN facilities. Nevertheless, as the sizes of cabinets change over time, as well as their contents, new experimental campaigns on modern electrical cabinets (such as those used in CERN) would be of great use to the whole field. On top of that only a single short campaign conducted in IRSN dealt with cabinets burning in confined areas (under ventilated conditions) thus this condition also deserves more attention in future works.

### **1.4.2 Vehicle fires**

In [12] a summary of experimental data collected from literature regarding single passenger road vehicle fires is shown. The summary is made by collecting the results from several large scale experimental campaigns on single passenger car fires done between 1980s and late 2000s. As intuitively expected, the total energy released and the time to peak HRR showed a trend of increasing with curb (total vehicle) weight. A drastic change over the last four decades in materials used in vehicles, especially plastic and composite content, is emphasized, increasing the fire severity. Thus, apart from the curb weight, another very important parameter to take into account is the vehicle age.

In [13] development of design fires for hard rock mines is presented. Each part of a mine is treated independently - from warehouse and workshop, to main ramp and cable shafts and vaults. Fires in heavy vehicles (service vehicles, drilling rigs and loaders) are analysed and deconstructed to individual partitions of the vehicles burning (seats, tyres etc.).

In [14], [15] and [16] results from fire tests on lithium – ion batteries typically used in electrified vehicles are presented and discussed. It is shown that batteries with higher state of charge (SOC) resulted in greater heat release rates and greater amount of toxic hydrogen fluoride gas produced, while SOC had way lesser influence on the total heat released.

In [17], full scale fire experiments were conducted on electrical forklifts. As they are commonly used for transporting heavy loads in nuclear facilities, the need for the experiments was obvious. Apart from the standard fire test results (Heat release rate, mass loss rate etc.) the outputs provide important thermodynamic and chemical characteristics of a forklift fire which can be useful for fire modelling.

#### **Conclusions for vehicle fires literature review**

It is observed that almost no research/experimental campaigns have been performed on small vehicles, thus a need for those is obvious. That could be avoided if small scale experiments on individual crucial components of small vehicles used in CERN and similar facilities are performed. If that happen to be the case, more precise design fires could be developed and thus all the vehicles present in CERN could be properly characterized in terms of the fire threat.

### 1.4.3 Particle size analysis

In [18] a new bench scale test was developed for investigating how different materials contribute to fire – particularly electric cables. The test consisted in a coupled mass loss cone, Fourier transform infrared spectroscopy, and electrical low-pressure impactor (MLC/FTIR/ELPI). This test apparatus makes it possible to simultaneously determine and characterize flammability parameters, released gases and smoke particles. Halogen-free flame retardant (HFFR) cables were tested. External heat flux varied from 25 to 75 kW/m<sup>2</sup>. Results are shown in figure 1 [18]. It was observed that cables had two peaks in Heat Release Rate (HRR) – one at the beginning of flaming, and another close to the flameout. Peak HRR remained constant regardless of the heat flux imposed. It was observed that biggest amount of CO<sub>2</sub> (97%) was released during the combustion, whereas the majority of CO (53%) was released after the flameout. It is shown that most of the particles fall into submicron range (<1 μm). It was interesting noting that, at 25 and 35 kW/m<sup>2</sup>, highest peak was observed for the 54nm particles, while in 50 and 75kW/m<sup>2</sup> imposed heat flux tests, highest peak was seen in 6nm particles.

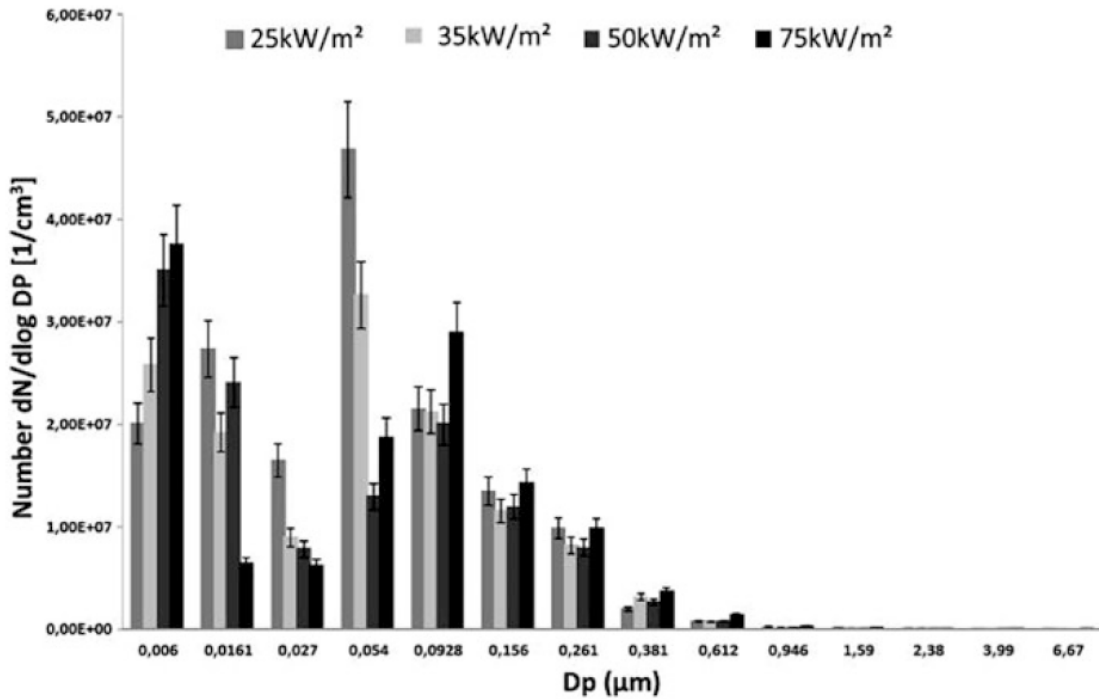


Figure 1 - Soot size distribution and number in the smoke of HFFR cables (MLC/FTIR/ELPI – 25, 35, 50, 75 kW/m<sup>2</sup>) [18]

Klippel, [19] gives a general classification of Particulate Matter (PM) dividing particles in nucleation mode – smaller than 100nm (also called ultra-fine particles); accumulation mode (100nm - 1 μm) and coarse mode (larger than 1 μm). It is emphasized that smallest particles usually have higher concentrations, but generally do not contribute significantly to the total mass. Process of formation of combustion particles is explained in detail – nucleation, condensation, coagulation and aging processes involving many complex chemical reactions. Particle emissions during combustion are divided into two groups – carbonaceous material (organic or elemental carbon)

deriving from unburnt fuel components, and inorganic material deriving from non-combustible components in fuel. Biomass and diesel particle formation is explained with note that major part of particles is again in submicron range, and the highest number concentration for diesel is in nucleation mode (<100nm). The usual bimodal particle size distribution is observed as it was previously established as a characteristic of aerosols in fire tests by [20]. The effect of dilution on particle formation when sampling aerosols is explained. Use of Differential mobility spectrometers for measuring particle mobility size distribution is introduced and explained, and DMS500 Fast Particle Analyser is used in experiments.

Wang, [21], tested PVC-insulated electrical wires studying ignition and characteristics of smoke particles formed during combustion. It was shown that smoke particle distribution fitted well the lognormal distribution. By analysing Transmission Electron Microscopy (TEM) images, it was observed that particle aggregates composed of many primary particles sized 50-80nm and the morphology was independent to the wire current. Time dependent Count Mean Diameter (CMD) and Geometric Mean Diameter (GMD) showed peaks at the start of the burning period, and later fluctuated in the range of 90-120 nm.

Slowik, [22] presents definitions for different “equivalent diameters” used to define submicron particles such as electrical mobility diameter ( $d_m$ ), volume equivalent diameter ( $d_{ve}$ ), aerodynamic diameter ( $d_a$ ), vacuum aerodynamic diameter ( $d_{va}$ ) etc. Also, instruments and methodologies using those diameters are presented. Relations between different equivalent diameters are given, with all the constraints they introduce. It was concluded that for irregular particles of standard density  $d_m > d_{ve} > d_a$ . It is shown that even if particle density and dynamic shape factor are not known, particle mass can still be calculated only from  $d_m$  and  $d_{va}$  measurements with an uncertainty factor of 2. Summary of different particle types and associated relations of particle density, material density and shape factor is given.

Butler, [23] explains soot formation and growth – from polycyclic aromatic hydrocarbons (PAHs) forming the smallest soot particles in the order of a few nanometres, to further creation coagulation and formation of particle agglomerates. It is found that generally smoke yield increases moderately with increasing fuel size. Nevertheless, for crude oil it was shown that increasing the diameter from 0.085 m to 2 m increased smoke production from 0.06 g to 0.13 g of smoke per gram of crude oil. The importance of the environment is emphasized – for six materials tested, smoke generation efficiency increased up to 2.8 times in under-ventilated conditions. In addition to that, smoke yields for wood cribs were found to be an order of magnitude larger for under-ventilated conditions in comparison to the well-ventilated case. It is also shown that as agglomerate size increases – the density of the particles decreases. For the majority of fuels tested, most of the smoke particles are in the submicron range (<1 $\mu$ m). Processes leading to losses in particle concentration are explained – particle sedimentation, particle diffusion and thermophoretic deposition. Also, estimation of how much smoke is deposited as a result of each process. Another interesting estimate is that 10-30% of smoke produced would be deposited within the room containing the fire over a period of 10 min to 30 min. Great effects of smoke aging process were demonstrated - over the 90 minutes of smoke being trapped in a chamber, concentration drastically decreased while the mean particle diameter increased.

## **Conclusions for particle size analysis literature review**

The literature review gave good insight in formation of smoke particles and their evolution through time. Also, key results from several interesting experimental campaigns are presented showing the importance of the imposed heat flux for the particle size distribution, then showing the independence of the particle sizes from the wire current, but also demonstrating the importance of the size of the pool for crude oil for example. It also gives a good overview for a reader to get a picture on the important knowledge relevant for testing smoke particles, and a possibility for a reader to go deeper in the referenced papers in order to get more detailed information on all mentioned topics relevant for aerosol analysis. It was observed that majority of tests done so far on smoke particle analysis have been based on impactors and other similar filter-based apparatus, thus more common use of fast particle analysers such as DMS500 is expected in future. The advantages of this device will be demonstrated and explained later in this thesis.

## **2 METHODOLOGY**

---

It is important emphasizing once more that as the results from Electrical Cabinets and Vehicle Fires were summarized only in a few graphs, it was author's decision not to separate them from the "Methodology" section, for the sake of easier following. Thus, the "Methodology" section contains methodology, results and discussion parts for both Electrical Cabinets and Vehicle Fires. On the other hand, as the results from Particulate Matter analysis were way greater, they will be presented independently in "Results and discussion" section.

### **2.1 ELECTRICAL CABINETS AND RACKS**

CERN is a complex and unique facility and this is true for the equipment installed in its premises. In many cases, standard, off-the-shelf equipment does not fulfil the specific needs of the Organisation. Therefore, most of the equipment used at CERN is custom made for unique purposes, which adds an extra complexity to assessing all potential hazards, including the fire hazard. Cabinets and racks used in CERN vary enormously in geometry, contents, distribution (a single cabinet, or 10 cabinets and racks combined in two rows (figures 2 and 3) and location (in control rooms above ground or in tunnels 100 meters below ground). Ideally, a design fire gives the total heat release rate over time for a certain scenario. Moreover, when all the input is predefined and well known (geometry of the room, combustibles materials and their heat release rates), creating a design fire is a bit easier for the engineer. In case of CERN, an envelope case or a worst-case scenario will always be treated, as an attempt to stay on the safe side, regardless of all the uncertainties.

The most likely ignition source in cabinets is a technical failure (short circuit, arcing, overheating etc.) [2], but the focus of this work will be assessing the consequences after the ignition has occurred.

#### **2.1.1 Theory – Design fires**

For most predictions of the consequences of fire, the development of the fire itself is used as an input. The input data are usually in the form of heat release rate versus time. [1] Babrauskas [24] emphasizes that heat release rate is the single most important variable in fire hazard.

As the assumption of this work is that the fire has occurred, the ignition phase will not be taken into account. This is because the time can vary from hours, due to overheating, to just a fraction of a second when ignition is caused by arcing [2]. Instead, fire will be analysed in three well-known stages – growth, steady and decay stages. In real, growing and ventilated fires, the initial fire development is nearly always accelerating. This would not be the case in smouldering fires, but that is out of the scope of this project. A simple way to describe the accelerating growth is to assume that the energy release rate increases as the square of the time. By multiplying time squared

by a factor  $\alpha$ , various growth velocities can be simulated, and the energy release rate as a function of time could be expressed as:

$$\dot{Q} = \alpha * t^2 \quad (5)$$

where  $\alpha$  is a growth factor (often given in kilowatts per second squared ( $\text{kW/s}^2$ )) and  $t$  is the time from established ignition, in seconds [25].

The growth phase lasts until the heat release rate reaches its peak value. It will be explained in the next section how the peak HRR value was determined. Fire now enters the steady phase and doesn't grow further as it's limited by HRR per unit area and extension of the burning surface. The steady phase ends when fire starts to decay i.e. cannot sustain the peak value anymore – either due to the lack of oxygen or lack of fuel.

When most of the fuel in an enclosure has been consumed, or the fire fails to spread to adjoining items, the rate of burning decreases generally due to the build-up of char. The onset of decay has not yet been defined and further research is needed for accurate prediction. In the absence of specific information, the heat release rate of the design fire may be taken to commence decay when 80 % of the available fuel has been consumed. [26]

In the decay phase, the HRR curve can be characterized according to the following exponential function [7]:

$$\dot{Q} = \dot{Q}_{(td)} \exp \left[ -\left( \frac{t - td}{\tau} \right) \right] \quad (6)$$

Where  $\dot{Q}_{(td)}$  is the heat release rate,  $td$  is the time at the start of the decay phase, and  $\tau$  is the decay time constant.

## 2.1.2 Design fires for electrical cabinets and racks

After a visit to some key CERN facilities, it is observed that electrical cabinets and racks can be distributed in any possible way – from a single closed cabinet to a set of 2 rows x N columns of combined racks and open and closed cabinets (figures 2 and 3). Therefore, an excel calculator for calculating design fire is developed in order to cover the common and possible fire scenarios.



Figure 2 - Open/closed cabinets + racks in a row – picture from one of CERN facilities



Figure 3 - 2x10 electrical cabinets – picture from one of CERN facilities

As the highest HRR values for cabinets are obtained with open doors, and the racks have similar content as the cabinets, an estimation is made that racks and cabinets with open doors will burn in the same manner. In other words, racks and open-door cabinets are treated as they were the same in calculations.

Obtaining the accurate heat release rate for a single cabinet is possible only if exact contents and specifications are known, as well as the precise geometry limits of the cabinet. As it was previously mentioned, and also as it can be seen in figure 1, cabinets and racks with their contents are

completely custom, and vary from case to case. Therefore, an estimation of the heat release rates from them will be made according to the values found in literature.

There have been several experimental campaigns on fires in electrical cabinets during the last decades. Results obtained in them vary due to differences in – sizes of cabinets, contents, ventilations conditions, modes of ignition etc. Calculations based on models proposed in the mentioned campaigns will be presented in “comparison with excel calculator” part. Electric Power Research Institute (EPRI) and U.S. Nuclear Regulation Commission made a document “Fire PRA Methodology for Nuclear Power Facilities” [11] as an attempt to summarize the state of art in the field. They gave values for peak HRR for open and closed cabinets, obtained as a 98th percentile from the previous experiments conducted in the US. The value of the peak HRR for one open cabinet (or rack) is taken to be 1000 kW, and for one closed cabinet is taken to be 500 kW as those are the values found in [11]. Exact values are – 1004kW for open, and 464kW for closed cabinets, but values of 1000kW and 500kW are taken for the sake of simplicity. Rounding down 1004 to 1000kW is acceptable as it is in the uncertainty range, and rounding 464 to 500kW, still leaves us on the safe side.

Heat release rates for single opened and closed cabinets are shown in the following figures:

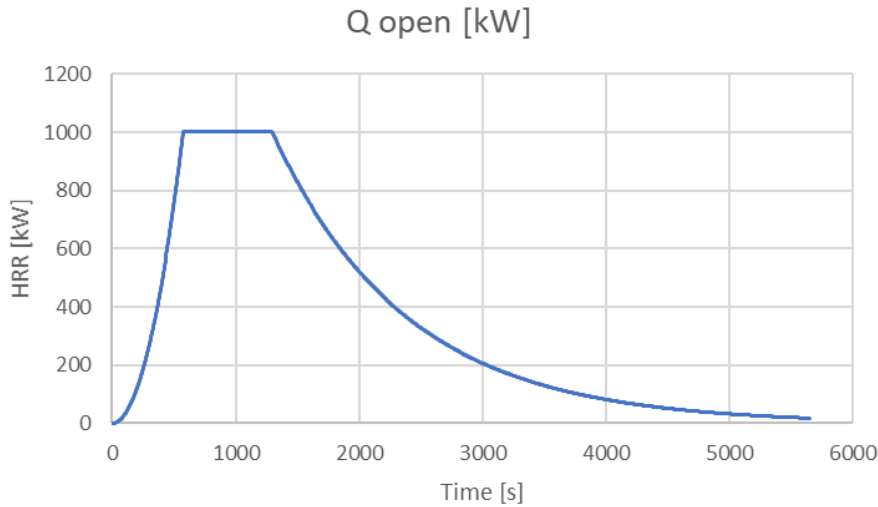


Figure 4 - HRR for open cabinet or rack

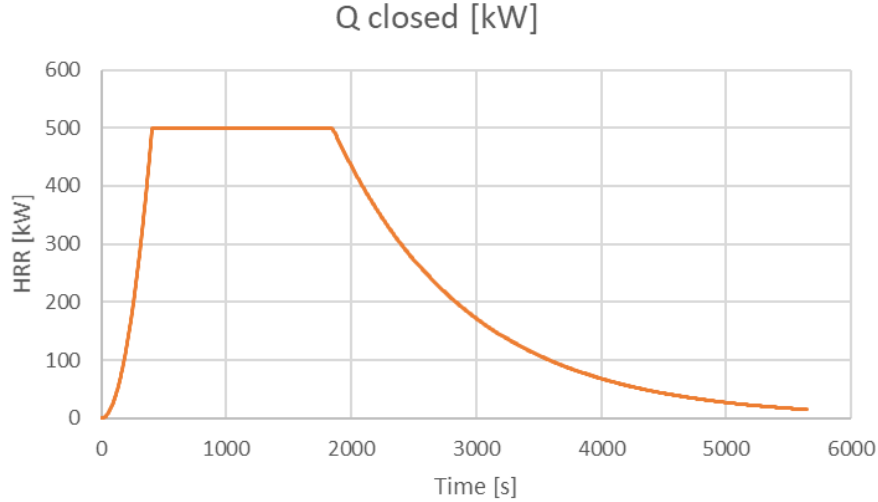


Figure 5 - HRR for closed cabinet

Growth phase is calculated according to  $\alpha \cdot t^2$  law, until it reaches the peak HRR value. The fire development in all the cabinet fire experiments was slow according to the NFPA classification [4]. Therefore  $\alpha = 0.003 \text{ kW/s}^2$ .

Integrating the HRR curves, and consequently dividing the obtained value by effective heat of combustion for PMMA (24MJ/kg), the total amount of fuel corresponding to these fires is obtained. Fire in a closed cabinet corresponds to 55kg of fuel, whereas fire in an open cabinet corresponds to 83kg of fuel. It will be explained below why PMMA is used as a reference fuel.

In the case where the amount of fuel is not known, the duration of burning at the peak heat release (steady burning -  $t_s$ ) will be taken to be  $t_s=12$  mins. [11] recommends  $t_s=8$  minutes to be taken, but due to the fact that some extreme cases of 17-20 min were observed, it is decided to be on the safe side, and take a 50% higher value than the recommended 8 mins, so  $t_s=12\text{min}$  is taken. In the case of closed cabinets, as their peak HRR is 50% smaller than peak HRR of open cabinets, it is assumed that duration of steady burning  $t_s$  will be 2 times longer than  $t_s$  of open cabinets. Thus,  $t_s$  for closed cabinets is taken to be  $t_s=24$  minutes. This is decided according to the engineering estimation that the same amount of fuel will take 2 times longer to burn if the peak HRR is 2 times smaller.

In the case where amount of fuel is known, peak HRR values will still be taken the same (1000kW for open and 500kW for closed cabinets), but time of steady burning is now calculated from the well-known relation:

$$\dot{Q} = \dot{m} * \Delta H_c \quad (7)$$

$$\dot{m} = \frac{m}{t} \rightarrow t_s = \frac{m * \Delta H_c}{\dot{Q}}$$

It is estimated from the graph for a single cabinet burning that 60% of the total energy is released during the steady state burning, therefore it is taken in calculations that  $Q = 0.6 * \dot{Q}_{peak}$

IRSN in [8] presented a summary of all experiments conducted on fires in electrical cabinets with details on configurations and giving major results. In CAB series of experiments, the influence of the fuel type on results was examined. Numerous plates made of polymethylmethacrylate (PMMA), polyvinylchloride (PVC) and polyethylene (PE) were used to simulate the fuel and they were tested in different proportions (e.g. 50% PMMA, 50% PVC, 0% PE, or 29% PMMA, 42% PVC, 29% PE etc.). Highest values for heat of combustion were obtained in the mentioned CAB series of experiments having a peak of 23.7MJ/kg in the case when 100% PMMA was used as a fuel.  $\Delta H_c$  will thus be taken to have a fixed value of 24 MJ/kg, as it is the worst case value obtained in experiments in [8].

Also, if the amount of fuel is known, the combustible fraction  $\chi$  needs to be specified. If it is estimated that all the contents of the cabinet are completely combustible, a value of 1 shall be chosen, otherwise a value between 0 and 1 shall be chosen. Amount of fuel refers to the amount of contents in one cabinet. As it was decided that peak HRR will always be 1000 kW for open and 500 kW for closed cabinets regardless of the amount of fuel - thus amount of fuel will only affect the duration of steady burning.

Decay is calculated according to equation (2). In [6], the decay time constants fitting the exponential functions describing the decay were in the range between 13 and 23 minutes. As no further data is available, it is decided to take the mid value, i.e.  $\tau = 18$  minutes.

Fire spread to the adjacent cabinet in 11-16 minutes according to the experiments done in [6] and [4]. To be on the safe side, it is assumed that the fire will spread to the adjacent cabinet after 10 minutes.

The mode of fire spread is conduction. Fire heats up the walls of the burning cabinet, that further heat up the wall of the adjacent cabinet, that finally heats up the cable bundle attached to it, which auto ignites after 10 minutes. In the experiments, the cable bundle coated in PVC was attached to the wall of the adjacent cabinet, as it is the worst-case scenario and results in the fastest fire spread. It is assumed that the cables ignite when they reach temperature of 250 °C. That temperature was taken as it was the maximum temperature at which the cable partially burned and partially deformed, indicating an approximate ignition level. This ignition temperature is in accordance with the range of decomposition of polyvinyl chloride, 200 – 300 °C. [6]

Worst case scenario is when a fire starts in a middle cabinet. In a simple one row case, fire would spread to two adjacent cabinets every 10 minutes.

In a more complicated case with 2 rows, after ignition of the first adjacent cabinets, further cabinets in the row opposite from the “fire cabinet” row would be heated by 2 cabinets at a time, thus it would take less than 10 minutes for each of them to ignite. An approximation of the times till the ignition of each of the cabinets is given in the following table. Numbers represent the time [min] at which each of the cabinets starts to burn – 0 being the initial “fire cabinet”, and in this case 50 being the last cabinet to ignite. The values shown are pure engineering intuitive approximation, with being cautious of staying on realistic “safe” side. It is observed that regardless of the number

of cabinets, after 50 minutes, there will be no difference between the time of burning in adjacent cabinets in each row, meaning that next two cabinets would ignite after 60 mins, then next 2 after 70 mins etc.

Arrows show how the heat is transferred from cabinet to cabinet.

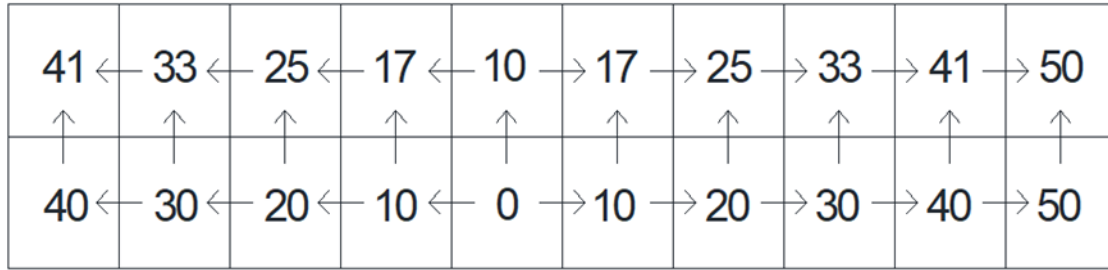


Figure 6 - Time (min) for fire spread to adjacent cabinets

Explanation on how to use the Excel calculator is given in Appendix G.

Finally, the following figures show the design fires for the extreme cases respectively – all open cabinets ( $2 \times 10$ ), all closed cabinets ( $2 \times 10$ ) and for the case of a combination of 8 closed and 4 opened cabinets. The curves could be smoothed, e.g. as simple  $\alpha \cdot t^2$  growth/decay curves with constant value for peak HRR during the steady burning period, in order to make it more easily usable in computational fluid dynamics software such as FDS.

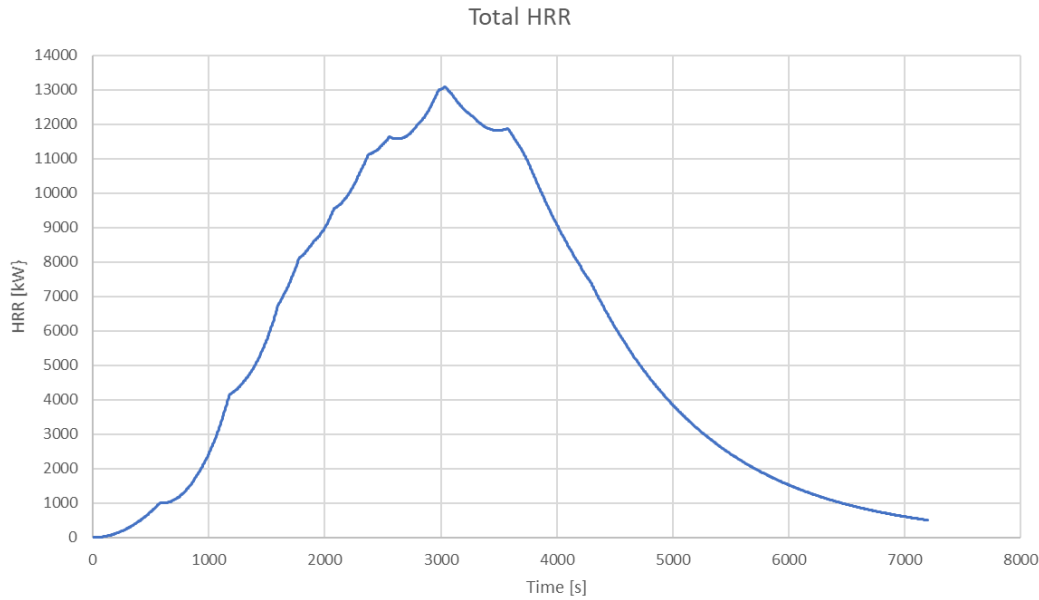


Figure 7 -  $2 \times 10$  Open cabinets (or racks) - worst case scenario

This fire corresponds to 1640kg of fuel (PMMA) in total, cca 82 kg per cabinet, which sounds like a realistic approximation.

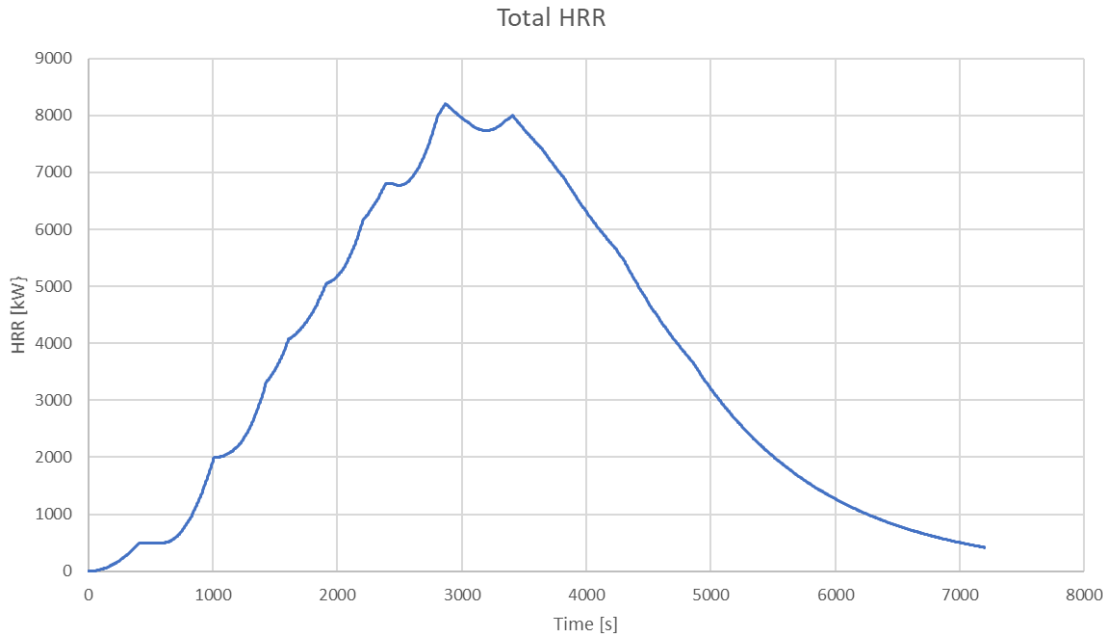


Figure 8 - 2\*10 Closed cabinets - extreme but most probable scenario

This fire corresponds to 1088kg of fuel (PMMA) in total – cca 54kg per cabinet.

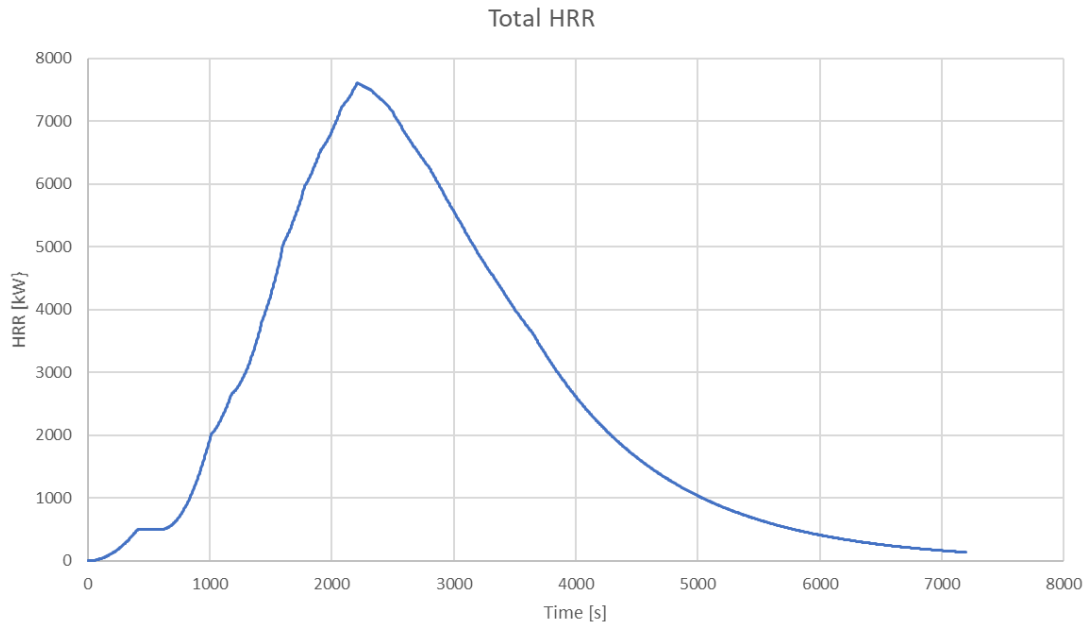


Figure 9 - HRR for 8 closed and 4 open cabinets (distribution 2C, 2O, 4C, 2O, 2C)

This fire corresponds to 769 kg of fuel in 12 cabinets, which corresponds to approximately 64kg per cabinet, which sounds like a realistic approximation.

All the values for total amount of fuel per cabinet shall be used just as a guideline and should be verified once the detailed contents of average cabinets are known.

### 2.1.3 Comparison of values used in Excel calculator with modelled values in France / Finland

As it was already mentioned in the literature review, several models have previously been proposed for obtaining the heat release rate of closed door cabinets.

First, in [4], a simple cabinet flow model assuming small vents and thus unidirectional flow is analysed and a dimensional equation for peak HRR in the following form is developed:

$$\dot{Q} = 4.3 * \sqrt{\frac{H}{\frac{3.3}{A_e^2} + \frac{1}{A_i^2}}} MW \quad (1)$$

After a new series of similar experiments, 10 years later, in 2004. Mangs proposed a similar but improved version of equation (1), including the combustion efficiency  $\chi$  that takes into account incomplete combustion:

$$\dot{Q} = 7.4 * \chi * \sqrt{\frac{H}{\frac{2.3}{A_e^2} + \frac{1}{A_i^2}}} MW \quad (2)$$

Finally, in [8] IRSN in 2011 have considered cabinets with vent areas that are non-negligible in comparison to the cabinet size, and also taken into account acceleration of the fluid due to its heating. Bernoulli equation yielded the following equation for the steady state mass flow rate:

$$q^* = \rho_\infty \sqrt{2gH} * \sqrt{\frac{1 - \left(\frac{T_\infty}{T_f}\right)}{\left(\frac{k_{in}}{S_{in}^2}\right) + \left(\frac{T_f}{T_\infty}\right) * \left(\frac{k_{out}}{S_{out}^2}\right) + \left[\left(\frac{T_f}{T_\infty}\right) - 1\right] * \left(\frac{1}{S_{cab}^2}\right)}} \quad (3)$$

Where  $\rho_\infty$  [ $\text{kg} \cdot \text{m}^{-3}$ ] is ambient air density,  $g$  [ $\text{m} \cdot \text{s}^{-2}$ ] is the gravity acceleration,  $H$  [m] is the distance between the vents of the cabinet,  $T_\infty$  and  $T_f$  are respectively ambient and flame temperatures,  $k_{in}$  and  $k_{out}$  are pressure loss coefficients at inlet and outlet (taken to be =2.8 as it is the value commonly found for turbulent flows [10]) and  $S_{in}$ ,  $S_{out}$  and  $S_{cab}$  [ $\text{m}^2$ ] are sectional areas of inlet, outlet and of cabinet.

The maximum heat released in the cabinet is determined from the oxygen available, i.e. from  $q^*$ :

$$\dot{Q} = q^* * \Delta H_{c,air} \quad (8)$$

where  $\Delta H_{c,air} = 3.144 \text{ MJ kg}^{-1}$  is a constant valid over a large range of fuels at standard conditions of pressure and oxygen concentration [8].

It is easily observable that in all three proposed equations, values of HRR strongly depend on the cabinet height. After a visit to CERN it was concluded that largest cabinets are 3 meters high,

which can be seen as an envelope case when determining HRR according to these equations. Peak heat release rates for a 3m high cabinet are calculated according to all three equations proposed, for variety of vent size ratios and the results are shown in the following table:

Table 1- Peak HRR values for various inlet/outlet ratios

Peak HRR [ kW ]		A outlet [ m <sup>2</sup> ]									
		0.01	0.02	0.03	0.04	0.05	0.06	0.07	0.08	0.09	0.1
A <sub>inlet</sub> [m <sup>2</sup> ]	0.01	49.39	71.49	80.07	90.41	104.89	116.40	125.48	132.65	138.35	142.91
	0.02	56.18	98.78	126.18	142.98	153.42	160.14	164.65	180.71	195.97	209.61
	0.03	57.78	108.32	148.17	177.72	199.08	214.47	225.68	233.97	240.21	245.00
	0.04	58.37	112.37	159.09	197.56	228.26	252.37	271.21	285.96	297.59	306.84
	0.05	58.65	114.41	165.03	209.30	246.95	278.36	304.29	325.58	343.07	357.45
	0.06	58.81	115.56	168.55	216.63	259.24	296.34	328.23	355.44	378.55	398.16
	0.07	58.90	116.27	170.79	221.44	267.60	309.02	345.73	377.97	406.13	430.63
	0.08	58.96	116.74	172.29	224.74	273.49	318.18	358.70	395.11	427.63	456.52
	0.09	59.00	117.07	173.34	227.09	277.75	324.95	368.49	408.31	444.50	477.22
	0.1	59.03	117.30	174.11	228.81	280.92	330.07	376.00	418.61	457.88	493.89

Mangs 2004

IRSN 2011

As it can be observed, peak HRR value for majority of inlet/outlet ratios is obtained using eq. 2 [6] – referred to as Mangs 2004, and a minority using eq. 3 referred to as IRSN 2011. When using eq. 2, combustion efficiency is taken to be  $\chi = 0.7$ , which is seen as an even conservative assumption as fires in closed cabinets are certainly well under-ventilated. As it can be seen in summary of cabinet experiments in [8], the most extreme case of ventilation sizes was  $A_{in} = 0.1\text{m}^2$  and  $A_{out} = 0.1\text{m}^2$ . In general vent sizes were way smaller. Thus, peak HRRs were analysed for the vent areas ratio of up to that size. It can be seen that even for the most extreme case when both inlet and outlet areas are equal to  $0.1\text{m}^2$ , the peak HRR value is 493.89 kW, which is still below the 500kW, which was the value taken as a peak HRR value for closed cabinets proposed by [11] and used in the Excel calculator. This validates the assumption of peak HRR for closed cabinets and further validates the excel calculator.

### Note for confined environment case

Cabinets burning in confined rooms were tested only in one experimental campaign in [8]. It was concluded that peak HRR value was weakly dependent on the confinement of the cabinet. On the other hand, mass loss rate, and burning duration were drastically smaller/shorter in confined burning case. This was due to lesser temperature differences, and thus smaller buoyancy. As a result, not all the combustibles were burned before the fire extinction occurred. Nevertheless, as peak HRR values remained unchanged, for the sake of staying on the safe side, potential confinement of cabinets used at CERN will not be taken into account, i.e. burning durations will be taken as if they were the same as in well ventilated case.

## 2.2 VEHICLE FIRES

After getting a first-hand insight into vehicles used at CERN, as observed during a visit, a literature review on current state of the art in vehicle fires was conducted with a goal to address fire risk imposed by CERN vehicles. Due to scarce literature relevant to CERN vehicle fires, but also due to impossibility to run tests, an attempt of characterizing only one type of vehicle commonly present in CERN will be made. Most of the literature related to vehicle fires deals either with passenger cars (buses) or with mining vehicles (drilling rigs, loaders etc) which all result in enormous heat release rates, and thus making comparisons and extrapolations between them and small vehicles present in CERN would be inappropriate. On the other hand, as there was a lack of data about electrical forklifts behaviour in fires, and as they represent a vehicle commonly present in many nuclear facilities, fire tests on electrical forklifts have been conducted by IRSN and results were presented in [17]. The major combustibles present in tested forklift were 4 tyres, cab (consisting of different types of polymer – wheel, seat, dashboard, cables etc.), hydraulic oil (15L) and electrical systems (engine, cables etc.) located in the compartment behind the driver seat. It is important noting that for safety reasons, the batteries were removed during tests.

Three tests were performed in [17] with three different ignition sources, still very similar behaviour was observed apart from the initial stage of the fire growth rate. Three stages in burning were observed in all tests.

The first stage (cab fire stage) is related to cab burning (the plastic board, the seat) combined with solid front tyres and the compartment of hydraulic system resulting in peaks in HRR of up to 1MW.

The first stage is followed by a decrease in HRR, but also in leak in hydraulic system. When oil heats up sufficiently, the second stage (oil pool fire stage) starts. Oil ignites and the flame spreads to the rear part of the vehicle igniting the rear tyres and the cables in the engine compartment resulting in HRRs of up to 800kW.

In the third stage (tyre fire) the fire decays, but tyres continue to burn for around 4 hours, with average heat release rate of 150-200 kW.

Graphical presentation of the whole burning process is shown in the following figure:

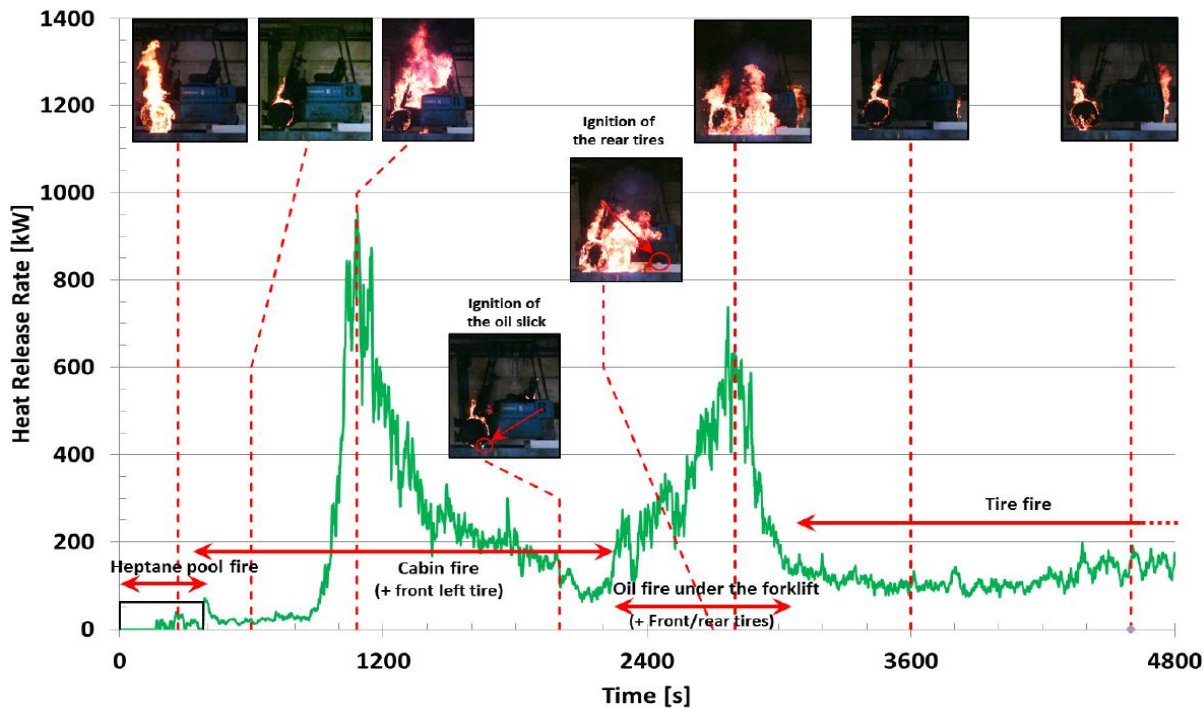


Figure 10 - Fire development in forklift fire, extracted from [17]

A quite common type of vehicle used in CERN is an electrical tractor shown in the following figure:



Figure 11 - Electrical tractor used in CERN

As the components of CERN electrical tractor are quite similar to the components of electrical forklift tested in IRSN experiments, HRR values shown in figure 9 can be used as good guidelines when making design fires that include electrical vehicles.

Several factors still must be taken into consideration. In IRSN experiments, the battery was taken out for safety reasons, thus the contribution of the battery in overall fire behaviour is unknown. Moreover, batteries used in CERN vehicles are lead-acid type, and no data is found in literature on behaviour of lead-acid batteries in fires. Also, many CERN tractors have reservoirs containing only 1-5 litres of hydraulic oil, while reservoirs in forklifts tested had 15 litres of hydraulic oil.

Another methodology to calculate the overall HRR of a vehicle in a tunnel or in an underground structure is proposed in [27] and could be potentially used for assessing fire behaviour of CERN vehicles. structure. The methodology basically sum up the individual HRR curves from each object of the vehicle by estimate when ignition between objects occurs. [27]

In [28], Ingason proposed value of  $0.20 \text{ MW/m}^2$  as good design value for heat release rate per exposed tyre surface. Still, the experiments conducted to obtain this value were done on large tyres, thus extrapolating to small tyres used in electrical tractors and similar vehicles introduces an uncertainty.

In [13] a test on a bus seat was conducted having a peak of around  $220\text{kW}$ , and a fire curve equation was obtained. Analogy between a bus seat and an electrical tractor seat could be made.

Overall, when making a design fire for a vehicle, precise HRR curves for each individual component of the vehicle should be known, and times of fire propagation from one component to another should be made. As more than 300 vehicles are being used in CERN, a separate campaign shall be made in order to obtain more precise insight into fire hazards of vehicles present there. Moreover, CERN will eventually start using lithium – ion batteries in electrical vehicles which introduce new hazards related to fire that have to be taken into account.

Further work in characterizing CERN vehicles fire hazard still needs to be done.

## 2.3 PARTICULATE MATTER ANALYSIS

The second part of this thesis was dedicated to smoke particulate matter analysis of three most common types of cables used in CERN, as well as two insulating oils used in transformers and klystrons. It is particularly interesting and important doing fire tests for the cables, as they are specifically manufactured for CERN. On the other hand, oils are commercial ones used for transformers, but still there is lack of information on particle size distribution from fires involving those oils.

In fire models, the accurate prediction of aerosol & soot concentrations in the gas phase, as well as aerosol & soot deposition thicknesses in the condensed phase, is important for a wide range of applications, including human egress calculations, heat transfer in compartment fires, and forensic reconstructions of fires. [29] Apart from those general applications, CERN in particular is interested in obtaining a deeper insight into smoke particle size distribution and concentration for a special reason. In case of a fire in one of CERN tunnels during experiments, it is expected that smoke particles, produced by burning activated materials, will be radioactive too and will further carry and deposit the radiation, which is a serious threat that has to be addressed and solved properly. For the sake of that, CERN has a need of obtaining a detailed smoke particle concentration and size distribution. This project will be used with the aim of validating the current state of art in Fire Dynamics Simulator (FDS), but also for further advancing and expanding the FDS code.

By not explicitly accounting for soot deposition on walls and surfaces, errors in soot concentration predictions in the gas phase can affect the calibration parameters for soot models. [29]

In [30] it is shown that FDS model overpredicted smoke concentration levels by the factor of 2 to 5 when comparing experimental and computational values found near the smoke alarms in a corridor. The discrepancy is said to be due to the large losses on the ceiling – up to 39% of the smoke produced. Another important finding of this work was a large discrepancy between reported small-scale soot yields and yields from larger scale fires (2 to 5 times smaller values from bench scale tests than the reported values).

One of the limitations of FDS is that the soot is currently represented in the model with a single (mean) particle size, and soot agglomeration is not currently considered. [29] Single (mean) particle case definitely wouldn't be a good approximation for cable fires as they show a bimodal distribution, which will be shown in this paper.

### 2.3.1 Experimental setup

As the goal of the experimental campaign was to assess general fire behaviour of the samples, but also their smoke particle size distribution, it was decided to couple the standard Cone Calorimeter produced by Fire Testing Technology (FTT) with the DMS500 Fast Particulate Analyzer. The setup is shown in shown in the following figures:

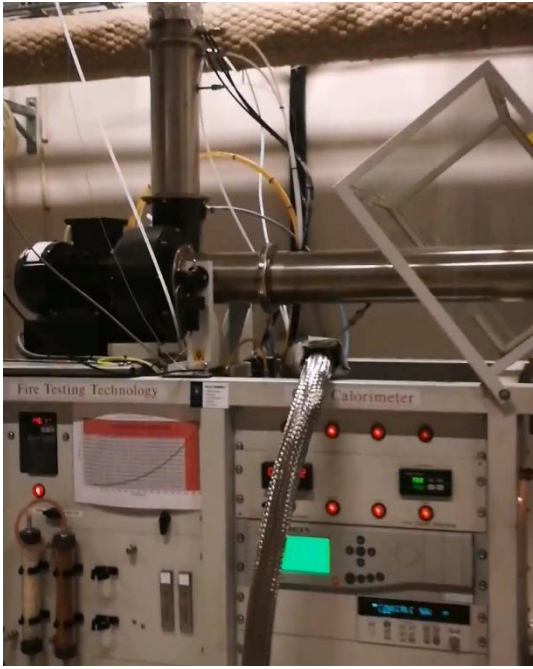


Figure 12 – Heated sample line connection to cone calorimeter



Figure 13 - Connection to the main control unit

### 2.3.1.1 Cone Calorimeter

The test method for the Cone Calorimeter is based on the observation that, generally, the net heat of combustion is proportional to the amount of oxygen required for combustion. The relationship is that approximately  $13,1 \times 10^3$  kJ of heat are released per kilogram of oxygen consumed. Specimens in the test are burned under ambient air conditions, while being subjected to a predetermined external irradiance within the range of  $0 \text{ kW/m}^2$  to  $75 \text{ kW/m}^2$ , and measurements are made of oxygen concentrations and exhaust gas flow rates. [31]

The major output from the cone calorimeter is heat of combustion. It is further correlated with the oxygen, CO<sub>2</sub> and CO measurements to obtain the value for Heat Release Rate, according to the equations proposed in the standard [31].

Another important property of the cone calorimeter is the smoke measurement option. It is based on the Bouguer's law which says that the intensity of light that is transmitted through a volume of combustion products is an exponentially decreasing function of distance. Smoke obscuration is measured as the fraction of laser light intensity that is transmitted through the smoke in the exhaust duct. This fraction is used to calculate the extinction coefficient according to Bouguer's law. The major output from this is the smoke production rate which is calculated as the product of the extinction coefficient and the volumetric flow rate of the smoke in the exhaust duct. [31]

Last, but not less important feature of cone calorimeter is the possibility of obtaining CO and CO<sub>2</sub> yields ( $\text{g/g}_{\text{fuel}}$ ) that are measured by SERVOMEX gas analysers, incorporated in the cone apparatus itself.

### 2.3.1.2 DMS500

The device used for sampling and analysing smoke particle matter is a Fast Particle Analyzer DMS500 (Cambustion Ltd., Cambridge, UK). Major feature of this device is that it tracks the Particle Number (PN) and measures the particles size distribution in the size range of 5nm -1 µm. For the sake of getting an idea of how precise this device is, it should be compared to a well-known and broadly used Dekati Low Pressure Impactor, that gives particle size distribution in 14 size fractions in the range of 16nm to 10µm, whereas DMS500 gives 38 size fractions (classes) between 5nm and 1µm ((4.87, 5.62, 6.49, ..., 749.89, 865.96, 1000 nm). Apart from being so precise, another even greater advantage of this device is that it does the measurements live – i.e. gives real time results. It represents a huge advantage in comparison to the traditional offline devices – impactors, soot samplers and other gravimetric, filter-based devices, that post-analyse the particles, allowing them to further coagulate, agglomerate and change their concentrations due to the aging process.

DMS500 works on the following principle: High voltage discharge is used to charge each particle proportionally to its surface area. Charged particles are introduced into a classification section with a strong radial electrical field. This field causes particles to drift through a sheath flow toward the electrometer detectors. Particles are detected at different distances down the column, depending upon their aerodynamic drag/charge ratio. Outputs from the 22 electrometers are processed in real-time at up to 10 Hz to provide spectral data and other metrics. [32]

Basically, particles are classified according to their electrical mobility. Smaller particles are more mobile, thus will deflect more easily after entering the electric field and will land on one of the first detectors, whereas larger particles being less mobile, will deflect a bit harder, and will thus travel longer distance before being deflected and consequently detected by the detector further along the classifier. The software uses the signal from those 22 detectors to calculate particle size and number spectrum.

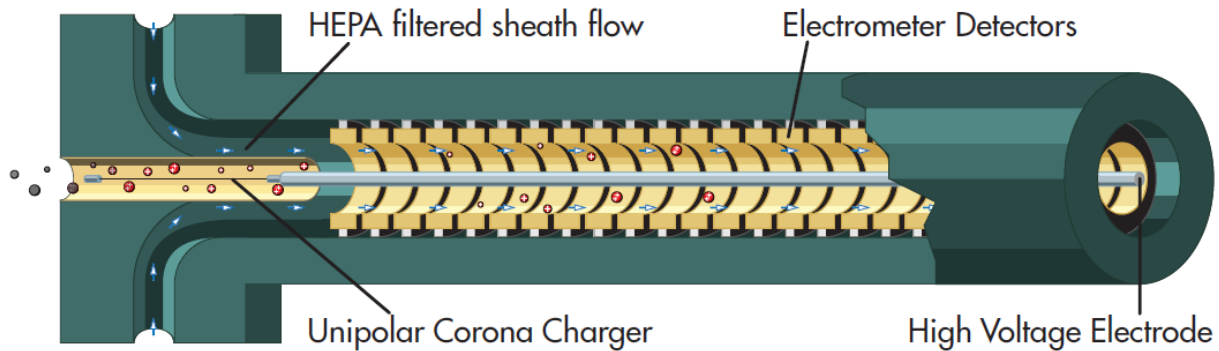


Figure 14 - Classification section - extracted from DMS500 manual [32]

The device takes sample with a heated sample line, that makes sure that no changes occur in the smoke sample as the product of thermal gradients. Besides that, device uses a two-stage dilution system, that prevents condensation and agglomeration at 1<sup>st</sup> stage and allows sampling from a wide range of particle concentrations with a high-factor 2<sup>nd</sup> diluter.

## 2.3.2 Samples preparation

### 2.3.2.1 Cables

As CERN already previously conducted experiments on the same cables as a part of the test campaign "CERN Cable Fire Tests" (CERN-CFT), the cables will be labelled in the same manner for the sake of easy comparison. Blue cables (C01), black cables (C02) and brown cables (C04) where C stands for CERN cable. Blue and black cables were regular multi conductor cables with thermoset insulation, whereas the brown cable was a coaxial cable with tight metal shield and a thermoplastic dielectric insulator around the core conductor (see figure 16).



Figure 15 - Cable types - C01, C02 and C04

The detailed specifications of all three cables are given in the following table:

Table 2 - Cables specifications

Cable no.	Manufacturer	Colour	Cable markings
C01	Draka	Blue	DRAKA 14W20 CERN MCA 14 IEC 60332-1 ZERO HALOGEN 09 3212577 405130804 3160 MT
C02	Elettronica conduttori	Black	ELETTRONICA CONDUTTORI - 13W19 - CERN PG5SJ - IEC 60332-3-24 - ZERO HALOGEN MT
C04	Draka	Brown	DRAKA 2016 CB 50 09 3414713 6111308426187 MT

For performing tests, cables need to be placed in a specimen holder. For the purpose of that, they were cut in pieces approximately 10.5cm long. For cutting the thicker cables (C01 and C02) hacksaw was used, while the thinner cable (C04) was cut with diagonal pliers. Cables were stacked

next to each other, wrapped in the aluminium foil and then placed into a specimen holder. In case of C01, 10 cables fit the holder, in case of C02, 9 cables fit, while in the case of this brown C04 cables, 16 cables fit. The role of the aluminium foil was to prevent molten plastic from dripping during the experiments, but also to prevent the pyrolysis gases from escaping on the sides of specimen assembly.

The sample holder consisted of the following pieces: frame bottom, ceramic insert, mineral wool, sample, grid, and frame top as shown in the following figure:

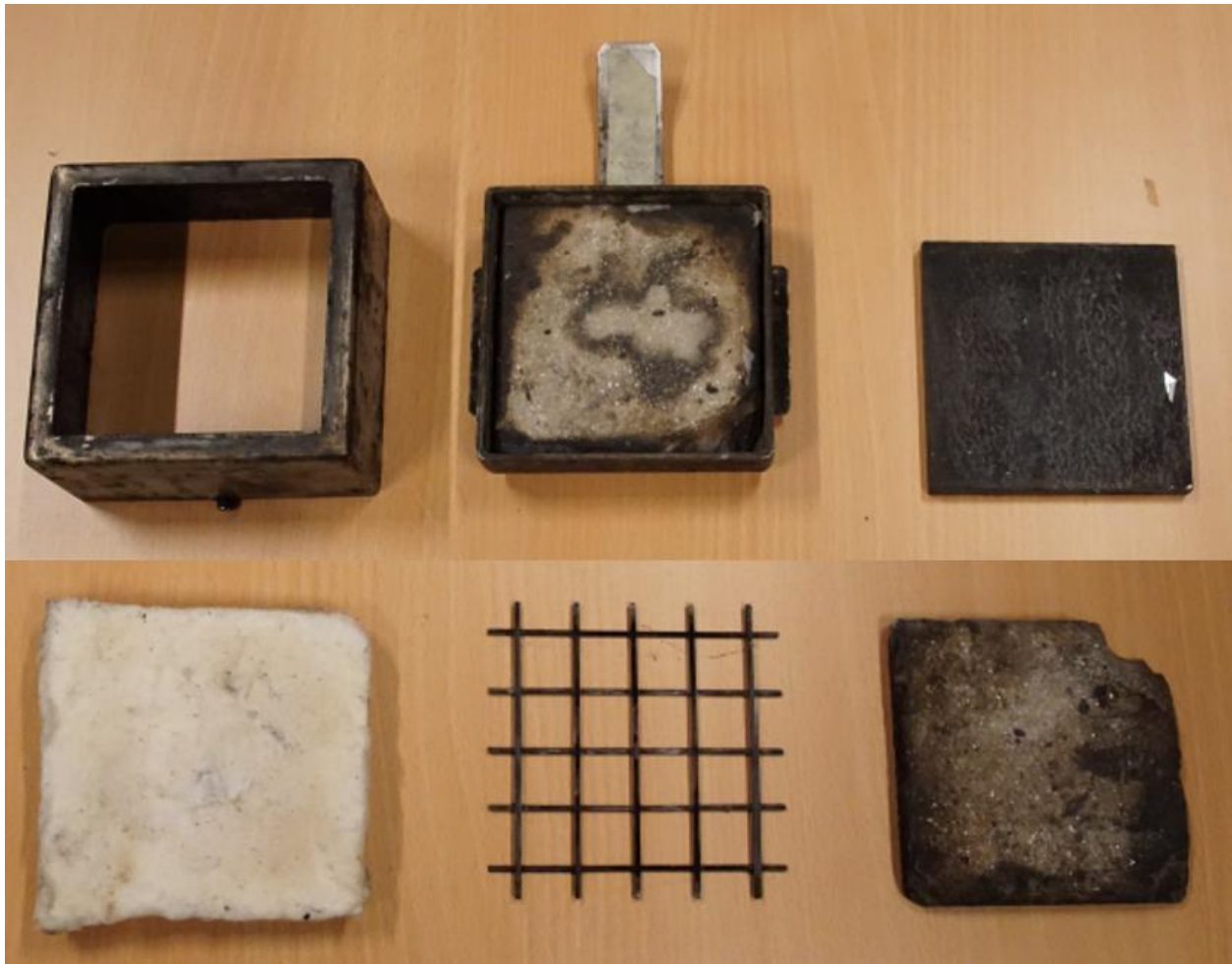


Figure 16 – Components of the specimen holder

For the thicker cables (C01 and C02) two ceramic inserts were used as a foundation of the specimen holder, while for the thinner cable (C04) three ceramic inserts had to be used in order to provide a good fit between the specimen and the frame. A layer of mineral wool was used on top of the ceramic inserts for providing some heat insulation below the sample but also to add extra tension by pushing the specimen towards the frame. As the distance between the cone heater and the specimen is crucial for performing precise tests, this step was very important. Cables wrapped in the foil were finally placed on top of the mineral wool, and eventually covered with a metal grid whose role was to prevent cables from swelling and bending during burning.

Complete sample ready for the test for C01 and C02 is shown in the following figure:

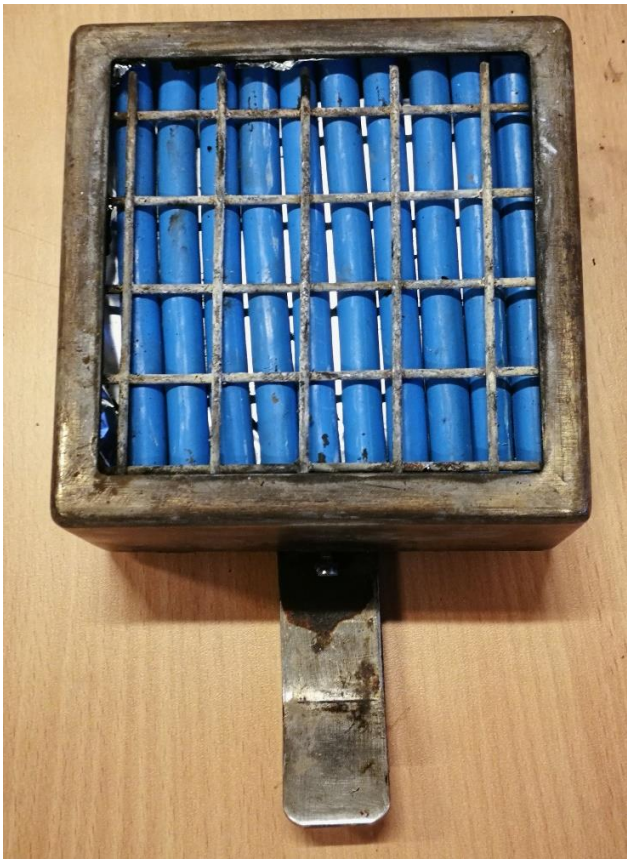


Figure 17 – C01 in sample holder – ready for the test



Figure 18 – C02 in sample holder – ready for the test

### 2.3.2.2 Oils

Oils tested were the most common ones used as electric insulating oils in transformers and klystrons present in CERN. Those were synthetic ester transformer oil MIDEI 7131 and Shell Diala S4 ZX-I having their flash points at 260 °C and 191 °C respectively. The sample holder used for testing oils was a simple squared shallow sample holder shown in the following figure:



Figure 19 – Sample holder



Figure 20 – Oil placed in the holder

The procedure for testing insulating liquids used in electrotechnical products in Cone Calorimeter given in British standard DD IEC/TS 60695 [33] was used. As it is recommended, 50 cm<sup>3</sup> of oil was used in tests. The supporter for the specimen holder of the cone calorimeter had to be lifted up until the prescribed distance of 23mm between the specimen and the heater was obtained.

### 2.3.3 Conducting the experiments

After turning on DMS500 and the cone calorimeter, and doing the routine of calibrating the cone calorimeter, before starting the tests, 30 mins had to pass as it is the stabilisation period time for the DMS500. Major parameters tracked (either directly measured or automatically calculated using certain needed measurements) by the cone calorimeter were – Heat Release Rate, Mass Loss, Effective Heat of Combustion, CO and CO<sub>2</sub> yields and Smoke Production rate, while DMS500 gave live outputs of particle size distribution (size and concentration).

Duration of combustion in cable experiments varied from approximately 28 minutes on average for blue cables (C01), then 47 minutes for black cables (C02) and around 13 minutes for brown cables (C04). On average, cooling down the sample holder after the experiments (washed with water for the sake of speeding up the process) and preparing new sample for test took around 20-25 mins.

Combustion times for oils tested were the following – approximately 12 minutes for Midel and around 8 minutes on average for Shell Diala oil. Cooling down the sample and preparing a new one for testing took 5-10 mins in total. Therefore, it is estimated that one cable test can be done every 50-70 minutes, while one oil test can be done every 20-25 minutes. According to DMS500 manual, the device can be used 24 hours/day, which leaves room for highly productive testing campaigns. Summary of times needed for conducting one complete test for each specimen are given in the following table:

*Table 3 - Times needed for conducting one full test*

Specimen type:	Avg. burning duration [min]	Cooling + preparing new sample [min]	CCA Total time for one test (burning + removal + preparing new sample) [min]
Blue cables C01	28	20-25	50
Black cables C02	47	20-25	70
Brown cables C03	13	20-25	35
Shell Diala oil	8	5-10	17
Midel oil	12	5-10	20

As in the first repetition blue cables (C01) did not ignite under the  $25\text{kW/m}^2$  of imposed heat flux, due to the lack of time, it was decided to test all the cables under heat flux of  $50\text{kW/m}^2$ .

On the other hand, oils were in the first trial tested under  $30\text{kW/m}^2$ , but due to quite aggressive burning, causing even a lot of spills, especially for the Shell Diala oil, it was decided to conduct further tests on oils under the heating power of  $20\text{kW/m}^2$ . After subjecting oil sample to given irradiance, it took on average 60s until ignition for Shell Diala oil, while it took on average around 180s for Midel oil to ignite. Samples have not been preheated in any of the tests.

Following figures show the samples during the tests:



Figure 21 – Blue Cables (C01) at the start of burning



Figure 22 – Blue cables (C01) after the test



Figure 23 - Shell Diala oil, burning process

### 3 RESULTS AND DISCUSSION

---

#### 3.1 CONCENTRATION GRAPHS – SHELL DIALA AND BLUE CABLES (C01)

A typical set of concentration graphs obtained from one test was shown in the following table (table 3). In this case, test was conducted on Shell Diala oil with the cone power of  $20\text{kW/m}^2$ .

Figure 25 shows particle concentrations over time for 1<sup>st</sup> and 2<sup>nd</sup> modes. It is clearly shown that 2<sup>nd</sup> mode (larger particles) are dominant.

Figure 26 shows total concentration of particles (sum of 1<sup>st</sup> and 2<sup>nd</sup> modes).

Figure 27 shows the average concentration from all runs. It is easily seen that the majority of particles belong to 2<sup>nd</sup> mode, which confirms the trend observed in figure 1.

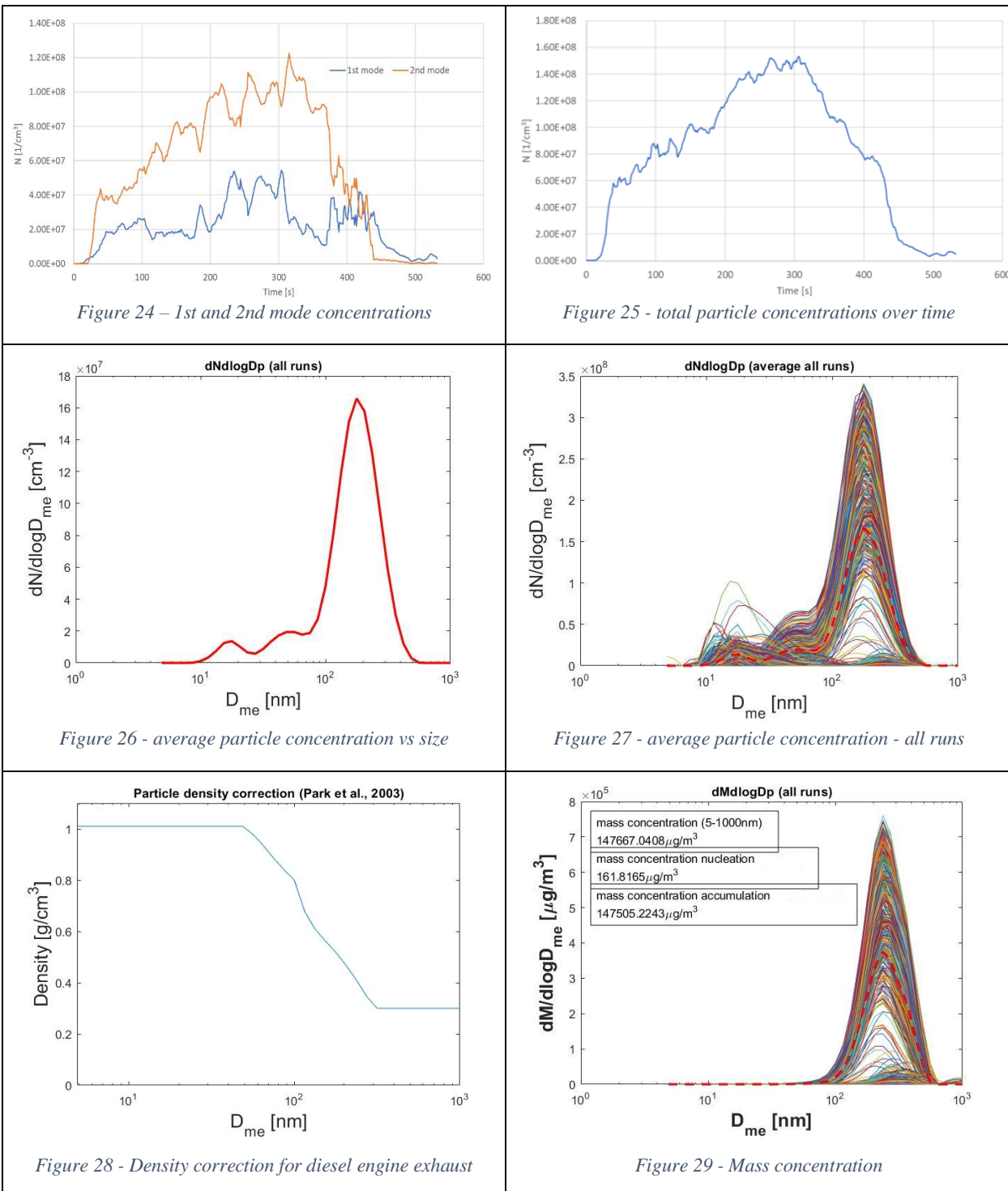
On figure 28, all readings from one test are shown, and the average is presented by the dotted red line. DMS500 operated at the frequency of 1Hz, thus we had 1 reading per second. For the sake of clarity, the red average line was shown independently on figure 6.

The concentration is expressed as a concentration size spectral density in  $\text{dN/dlogDp}$  with units of  $(\text{N} \cdot 1/\text{cm}^3)$ . When representing regular concentration (N) vs particle diameter (Dp), it can be tricky and even misleading comparing the graphs and values obtained with different instruments working with different resolutions. The solution to this problem is found when using normalized concentration ( $\text{dN/dlogDp}$ ). With normalized concentrations the concentration values at the mode will be similar even on instruments with very different resolution. [34] DMS500 uses 16 channels per decade resolution, meaning that in order to get the total particle number N, value for  $\text{dN/dlogDp}$  should be divided by 16. More details about that can be found in Appendix D of the main manual for DMS500 [35].

In [36], aerosol particle mass analyser was used to measure the mass of diesel exhaust particles. They managed to determine the effective density and found that it decreases as the particle size increases. By observing TEM (transmission electron microscopy) images, they realised that this phenomenon occurs because the particles become more highly agglomerated as size increases. The particle density correction model for diesel exhaust particles is shown on figure 29. By using density of diesel exhaust particles, mass concentration for our tests was calculated and the result is shown in figure 9. Therefore, it is important to have in mind that the mass concentration results are not accurate, as mass of smoke particles and their density for cables and oils used were not known, thus the values of diesel exhaust were used as an approximation.

Although there are quite a lot of readings in the 1st mode (figure 28), they are not visible at all in mass concentration graph (figure 30), simply because larger particles are way heavier and thus have greater impact on mass concentration.

Table 4 – Shell diala – concentration graphs



A same set of graphs is shown in table 4 for one type of cables – the blue cables (C01). First thing that can be observed from the particle concentration graphs (figures 31 and 32) is that burning was not as steady as with the oils. Knowing the structure of cables, and after observing the experiments, this can be justified in the way that at first the sheath was burning, when majority of particles were in the 1<sup>st</sup> mode, but approximately after 500<sup>th</sup> second the insulation started burning resulting in another peak in total concentration, with more 2<sup>nd</sup> mode particles during this period of burning.

Table 5 - Blue cables (C01) - concentration graphs

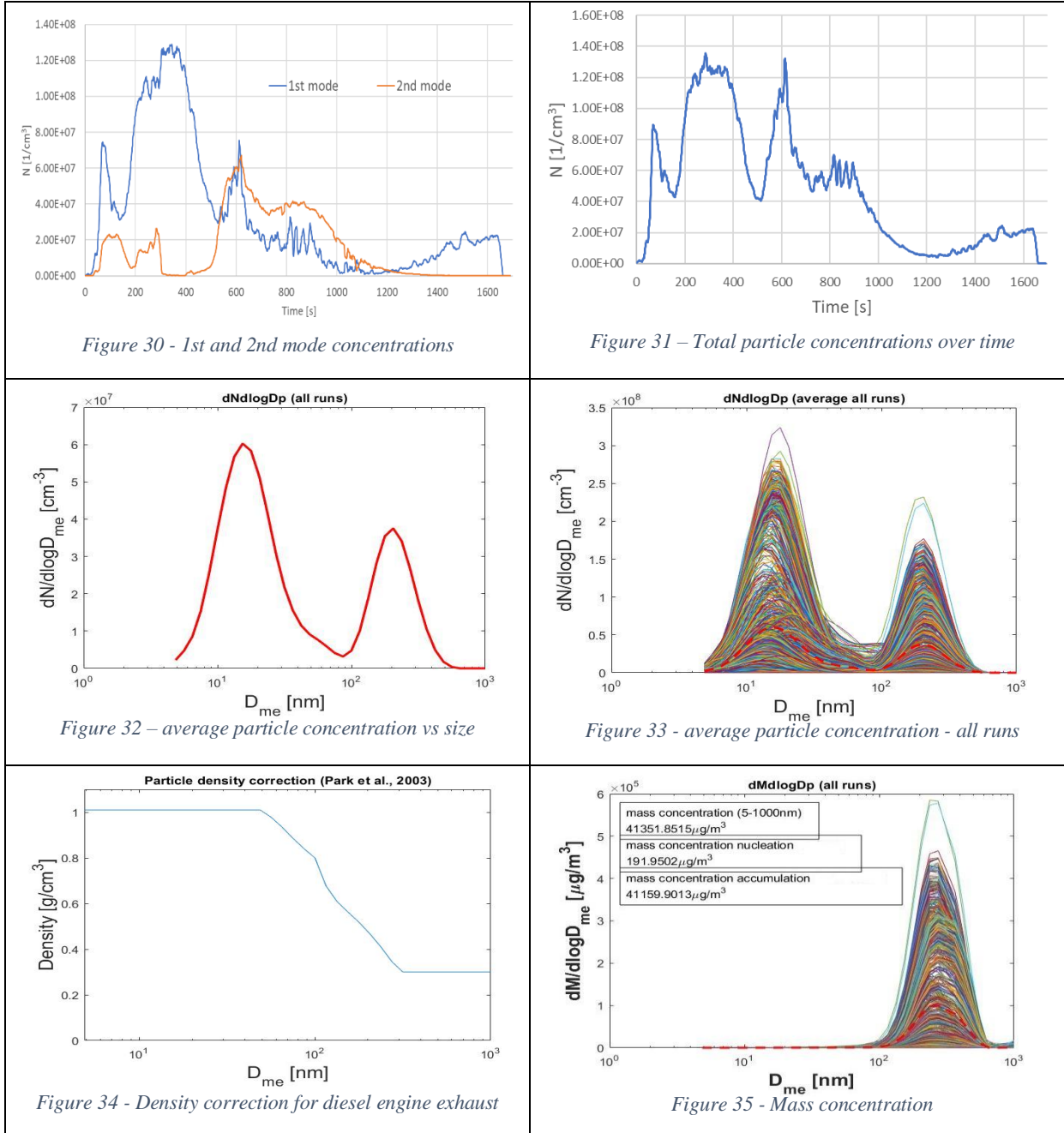


Figure 33 is again in good accordance with figure 31, demonstrating clear bimodal particle distribution, with higher particle concentration belonging to the 1<sup>st</sup> mode.

Finally, when comparing figures 34 and 36, it is even more clear than in Shell Diala oil case, that although there is a huge number concentration in 1<sup>st</sup> mode particles, they are practically invisible in the mass concentration graph as they are way lighter than the larger 2<sup>nd</sup> mode particles.

Concentration graphs for Midel oil, brown cables and black cables are given in Appendix A.

### 3.2 MAJOR GRAPHS FOR ALL SPECIMENS

A very interesting and unusual behaviour was observed when testing Midel oil. In all 3 tests, sudden peaks of concentration were observed at the very beginning and at very end of burning as it can be seen in figure 37.

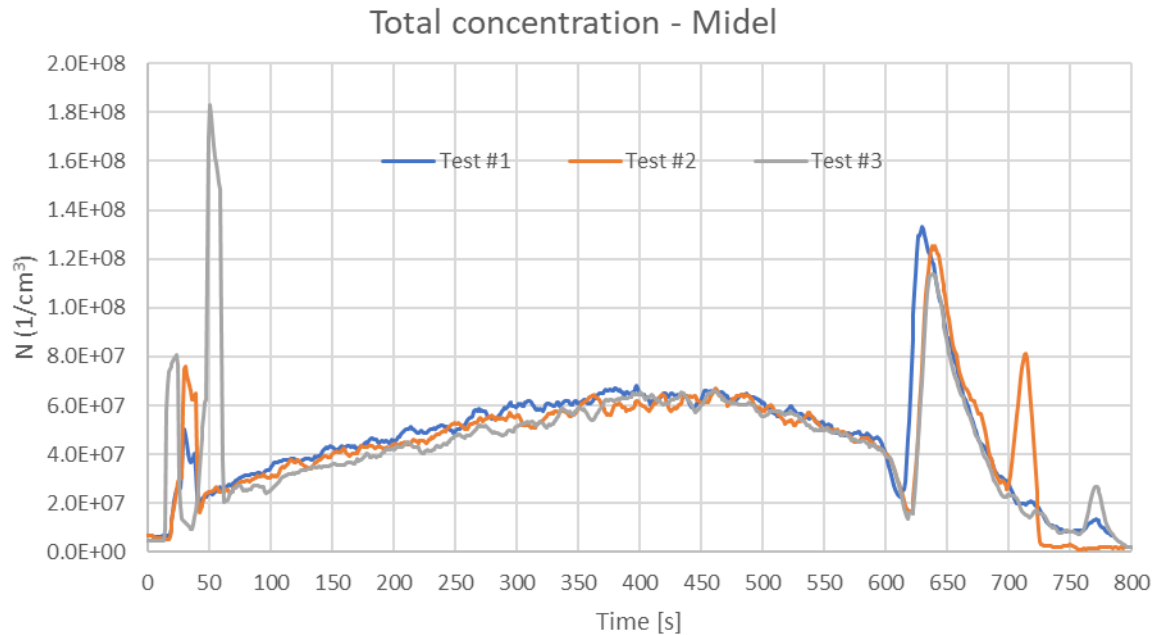


Figure 36 - Concentration in all 3 tests

This might be explained as if there is massive accumulation of volatiles during the heating phase that are suddenly released when the fire starts. The peak in the end of burning can maybe be explained in the following way: as there is less and less oil left, the “free” or “dry” area of the sample holder gets larger, thus it heats up more efficiently, and maybe suddenly causes more intense burning which results in great particle concentration peak. This is a pure guess, and this phenomenon needs to be studied further in order to be understood better. Also, it would be expected if this was the case, that the smoke temperature, measured with a thermocouple located in the main duct, shows a peak towards the end of burning, but that is not the case. Unfortunately,

videos of experiments are not available, therefore peaks cannot be compared with visual observations which could maybe give a better insight into this phenomenon.

On the other hand, HRR values showed great accordance and way more “calm” graphs for both oils, as it is shown in figure 38 on the example of Midel.



Figure 37 - HRR for all 3 tests – Midel oil

Solid accordance in HRR measurements in repeated tests was shown even in cables. An example for blue cables can be seen in figure 39. First peak represents burning of the outer sheath. A steady period roughly between 200s and 400s represents the time when heat is slowly penetrating through the metal sheath. Eventually fire catches the inner sheath of wires, that is seen as the second major peak, that in general in all cables shown the greatest peaks during the whole burning period.

HRR graphs for all tests for Shell Diala oil, Black Cables (C02) and Brown Cables (C04) will be given in appendix E.

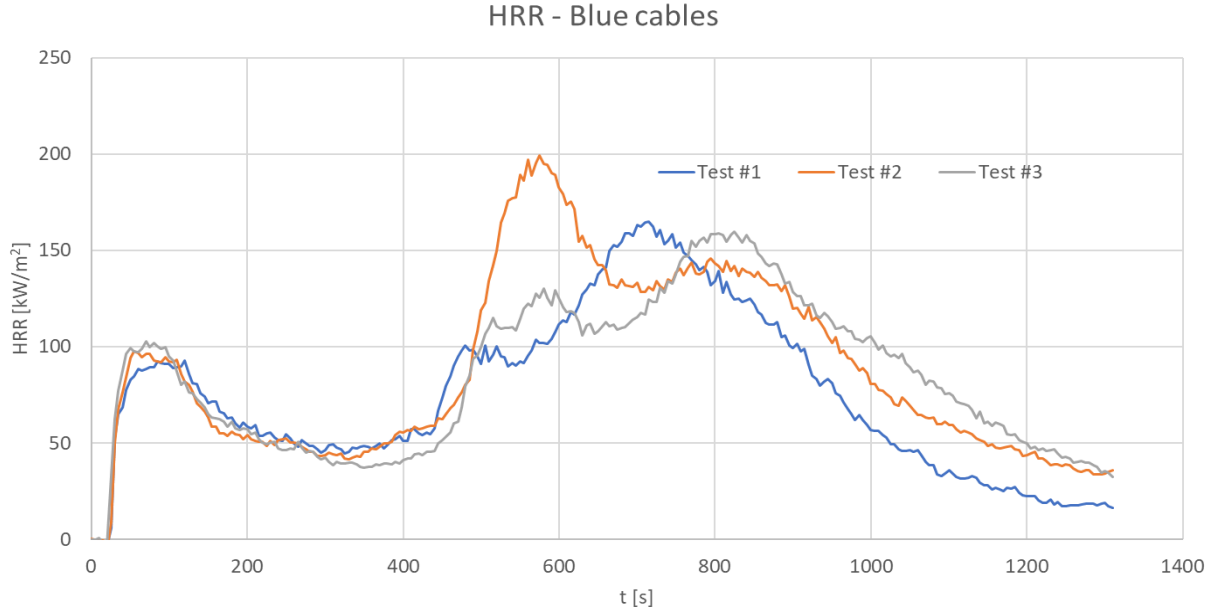


Figure 38 - HRR for all tests - Blue Cables (C01)

It was interesting observing that overall all 3 cable types showed higher concentrations in nucleation than in accumulation mode. Typical graphs showing that for brown cables (C04) are shown on figures 40 and 41.

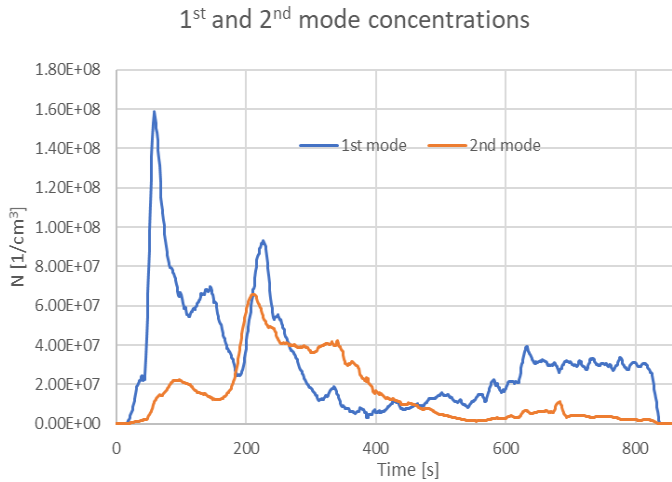


Figure 39 - 1<sup>st</sup> and 2<sup>nd</sup> mode conc. – brown cables (C04)

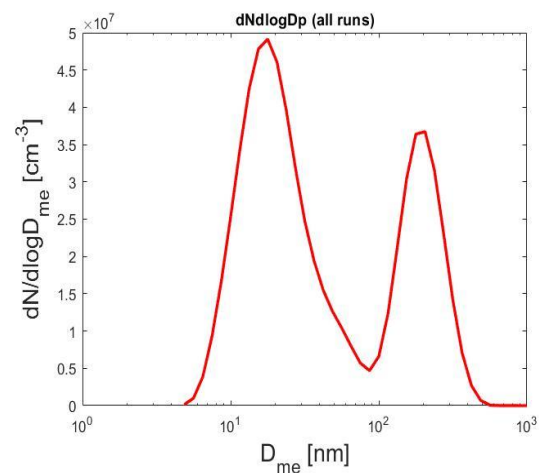


Figure 40 - Bimodal distribution - brown cables (C04)

It is important keeping in mind that all the cables tests were conducted using  $50\text{kW/m}^2$  cone power, and there is a possibility that particle size/concentration distribution will not be the same when other cone powers are used, just like it was the case in electrical cable tests conducted in [18]. In

[18], testing cables under lesser cone powers ( $35$  or  $25\text{kW/m}^2$ ) resulted in greater average particle size.

Another very peculiar behaviour is noticed in black cables. In all 3 tests, there was a sudden extreme release of 1st mode particles, as it can be observed in figure 42. It might be again explained as if there is maybe a high concentration of pyrolysis gases that suddenly burn at the beginning of flaming, and thus result in the observed peak.

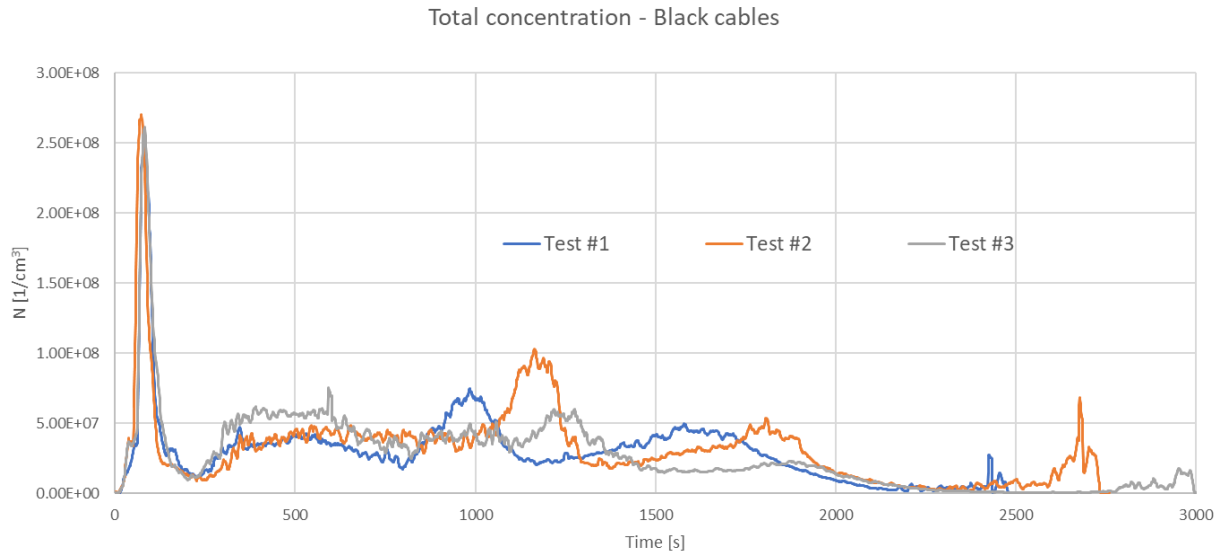


Figure 41 - Total concentration for all 3 tests - black cables (C02)

Comparing concentration vs time distribution for all three cable types, it can be stated that they generally follow roughly similar trends. Nevertheless, a very unpredictable burning nature can be observed both in the number concentration peaks that vary from  $1*10^8 / \text{cm}^3$  to almost  $1.4*10^8 / \text{cm}^3$ , but also in burning duration that varies roughly from  $1400 - 1650$  seconds in the case of blue cables, as it can be seen in figure 43. A sudden peak in the end of test #3 is believed to be noise, still as videos are not available, and as not enough repetitions could be performed, it is still shown in the graph in order to be further tested in future.

Total concentration graphs for Shell Diala oil and Brown Cables (C04) are given in appendix D.

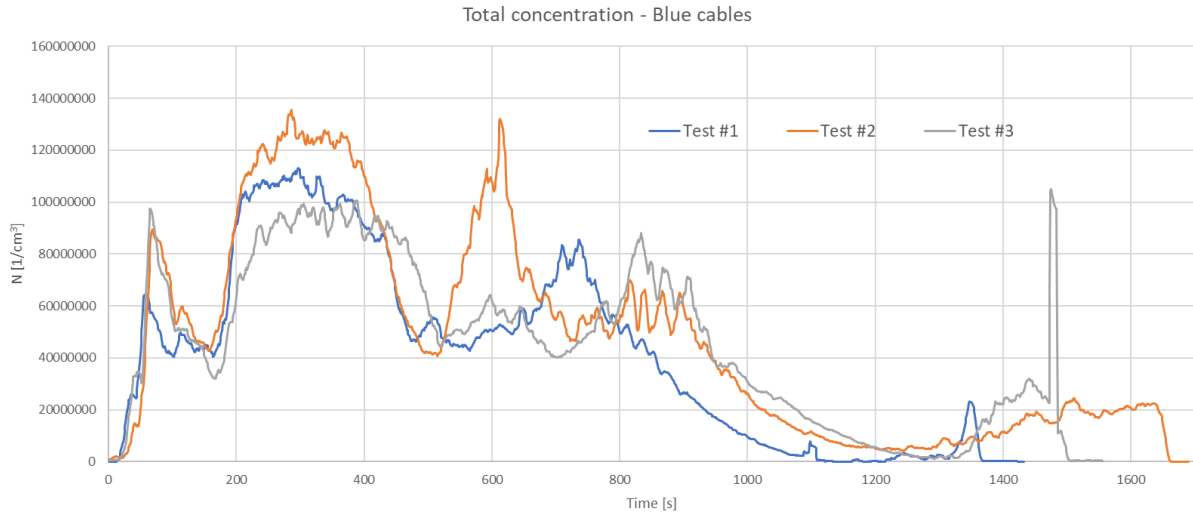


Figure 42 - Total concentrations - Blue cables (C01)

Accordance of heat release rate and total concentration of particles was as expected matching greatly for oils, as they burn more steadily than the cables. It can be observed in figures 44 and 45. Apart from the two extreme peaks in concentration for Midel oil, the trends of HRR and concentration lines match pretty accurately.



Figure 43 - HRR & Total concentration - Midel

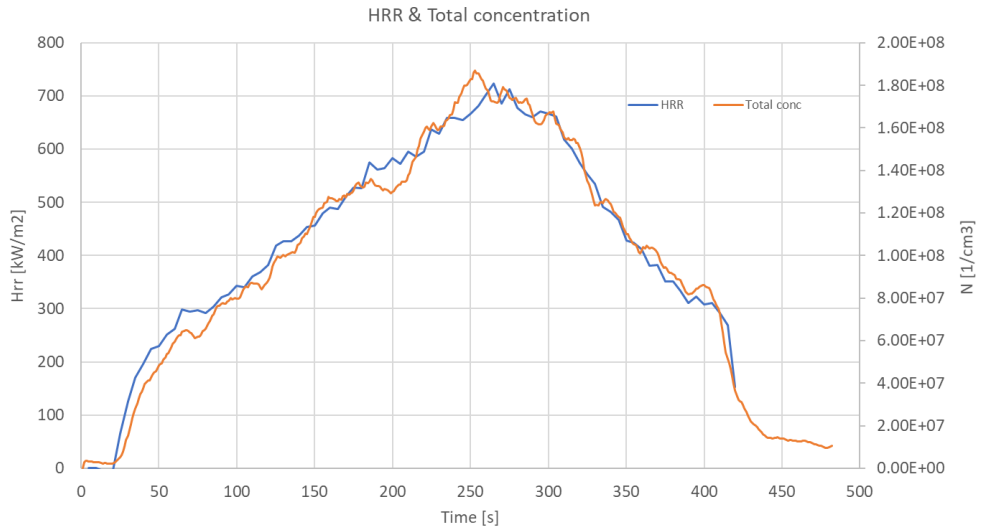


Figure 44 - HRR & Total concentration - Shell Dlala

Unlike for the oils, matching of HRR and concentration trends for cables was pretty poor as it can be seen in figures 46, 47 and 48. Nevertheless, a slight accordance is visible and some observations can be made.

For blue cables (C01), it can be observed that the highest and longest peak in total concentration occurred during the “steady” phase between the two peaks, meaning that a lot of pyrolysis gases were released at that period.

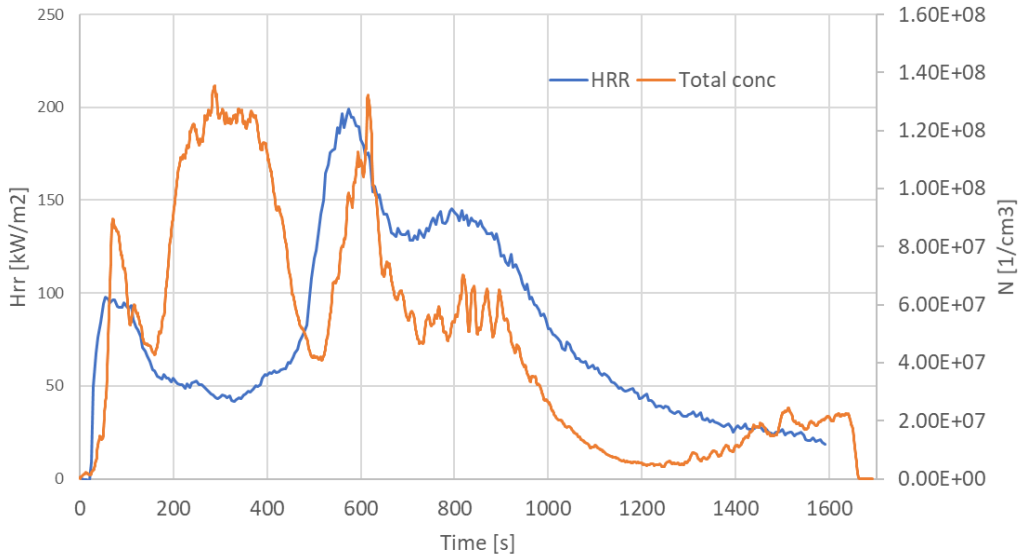


Figure 45 - HRR & Total concentration - Blue Cables (C01)

No correlation between HRR and total concentration could be observed when testing black cables (C02).

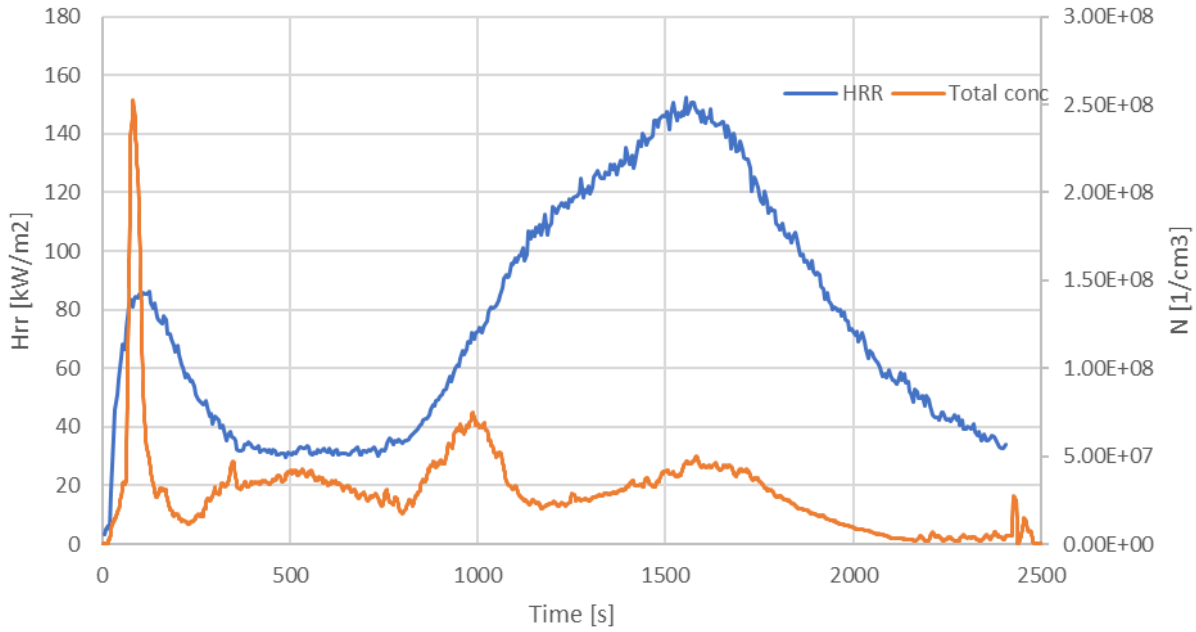


Figure 46 - HRR & Total concentration - Black Cables (C02)

Looking at brown cables burning, it is interesting seeing the increase in concentration after the flameout meaning that a lot of volatiles were released even after the burning period. End of blue line (HRR) represents the moment of flameout. The moment when orange line (Total conc) drops to zero is the moment when sample was removed from the holder. It would be interesting seeing for how long the volatiles would continue releasing after the flameout if the specimen was not removed.

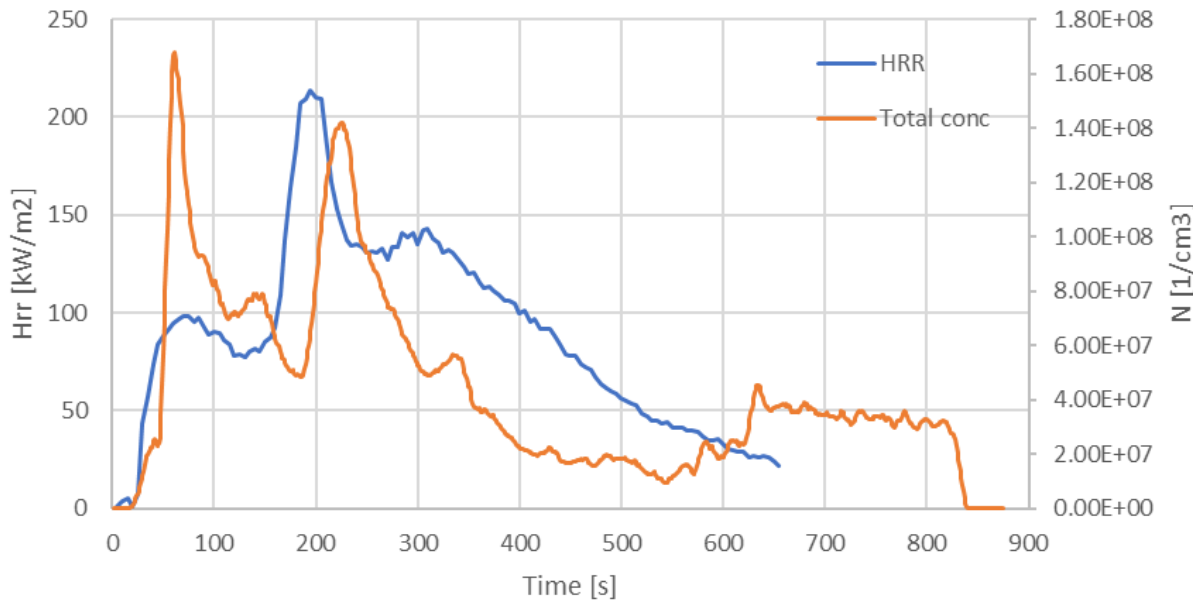


Figure 47 - HRR & Total concentration - Brown Cables (C04)

It is interesting observing how the effective heat of combustion fluctuates and follows the trend of HRR. Materials such as cables, that have more than one mode of degradation show more “peaks” in HRR while burning, and consequently accordingly variable effective heat of combustion (EHC). EHC is obtained by dividing HRR (obtained by oxygen depletion method) and Mass Loss Rate (which is a direct measurement). As cables have several materials involved in their structure – sheath, insulation, fillers etc. each of them having their specific EHCs, a mixture in behaviour results in HRR and EHC graphs not according perfectly, as they would in case of regular materials with one mode of degradation (e.g. oils).

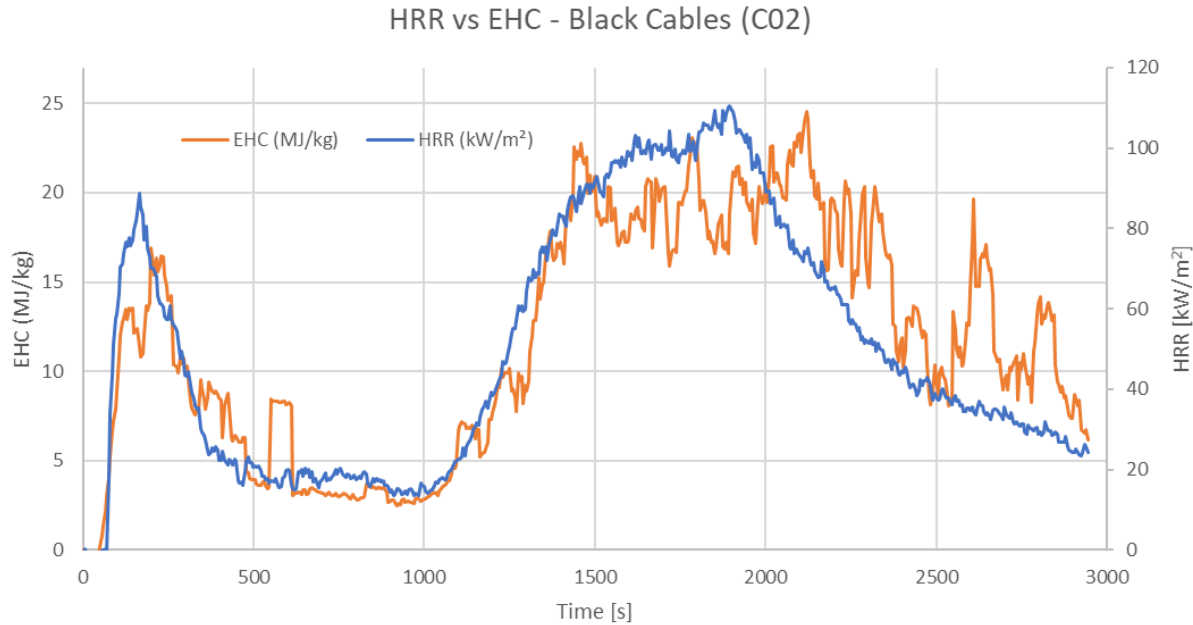


Figure 48 - Heat Release Rate vs Effective Heat of Combustion - Black cables (C02)

A comparison between mass loss rate and total concentration was made as an attempt to check if there is a correlation between the two. Apart from the first extreme peak in concentration that matches the first peak in mass loss rate, no further trends and thus conclusions could be made.

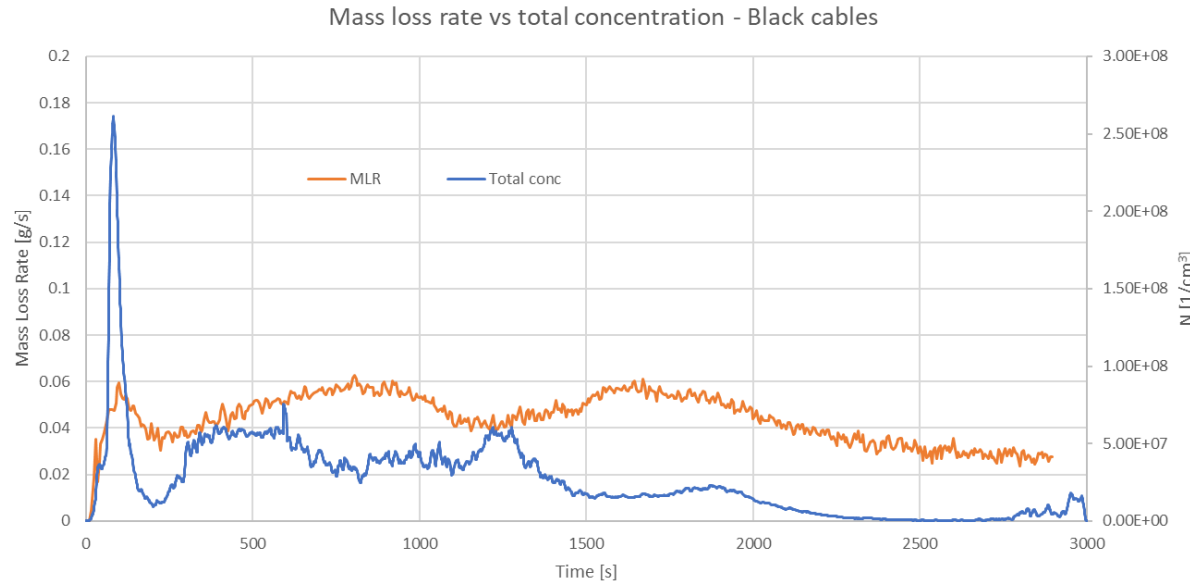


Figure 49 - Mass loss rate vs total concentration - Black cables

A very interesting phenomena is observed when comparing results for smoke production rate (SPR) measured with cone calorimeter with particle concentrations. SPR ( $\text{m}^2/\text{s}$ ) is obtained as a product of the volumetric flow rate of smoke ( $\text{m}^3/\text{s}$ ) and the extinction coefficient ( $1/\text{m}$ ) of the smoke at the point of measurement. Extinction coefficient is given as natural logarithm of the ratio of incident light intensity to transmitted light intensity, per unit light path length. [37] Thus, in simple words, greater attenuation of laser results in greater smoke production values. When comparing concentration values and smoke production rate for cables, it is observed that SPR almost perfectly accords with 2<sup>nd</sup> mode concentration particles, as it can be observed on example of black cables on the following figure:

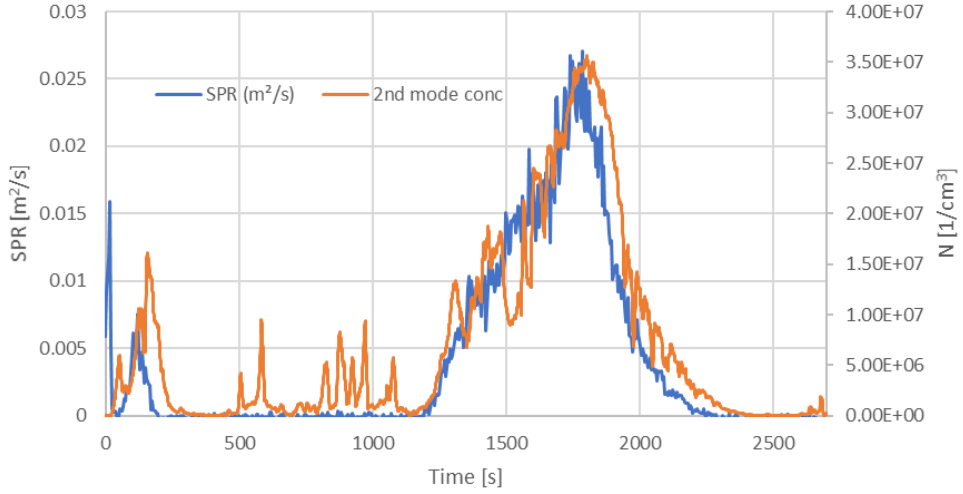


Figure 50 - Smoke production rate vs 2nd mode concentration - Black cables

On the other hand, when comparing SPR and 1<sup>st</sup> mode concentration particles, it can be observed that they do not agree at all (figure 52). Default Cone Calorimeter operates using a laser with red light having its wavelength around 630nm, which is apparently too high to be affected by the tiny smoke particles. This demonstrates the cone calorimeter's incapability of "capturing" all the smoke produced if the default version is used. This limitation should be taken into account when dealing with cone calorimeter in future. This can maybe be solved when using instead lasers with lesser wavelengths, e.g. ultraviolet light lasters.

Same behavior was observed in other cables tested. SPR values matched greatly with 2<sup>nd</sup> mode concentration, while 1<sup>st</sup> mode particles although sometimes having extremely high concentrations, were practically "invisible" on smoke production rate measurements. SPR vs concentration graphs for other cables are given in Appendix F. As oils had shown steadier burning, and dominance of 2<sup>nd</sup> mode particles, this behavior cannot be clearly demonstrated with graphs, thus it will not be shown in the Appendix F

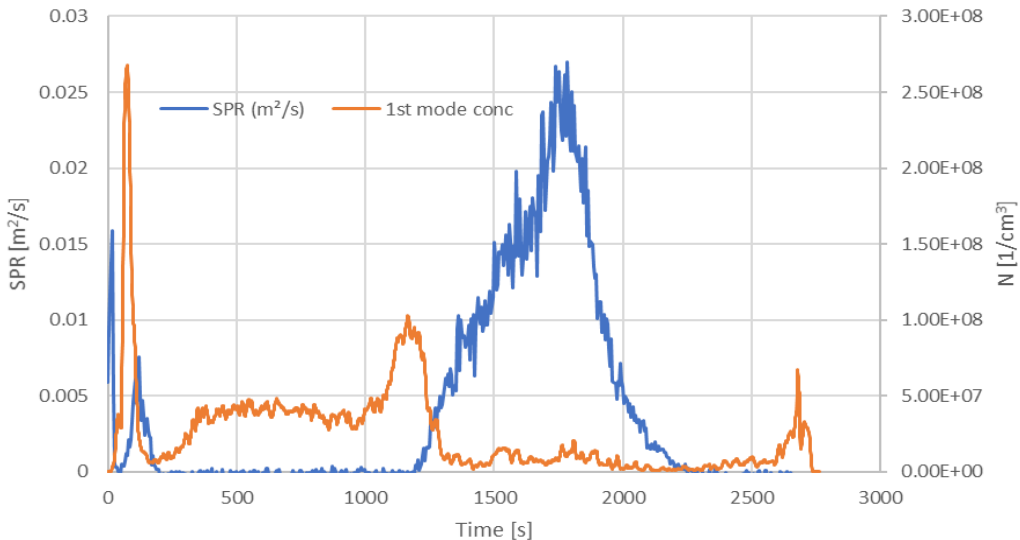


Figure 51 - Smoke production rate vs 1st mode concentration - Black cables

### 3.3 3D PLOTS

The following 3D plots show particle concentration of different sized particles variation over time for Blue Cables (C01) and Shell Diala oil. Bimodal distribution of particles is more than obvious. 1<sup>st</sup> mode burning in the first part of burning represents burning of the outer sheath, and the 2<sup>nd</sup> mode particles present in second part of burning represent burning of wires sheath. It is obvious that main (outer) cable sheath and inner wire sheath are made of different materials. 3D plots for Midel oil and other two cable types are given in appendix B.

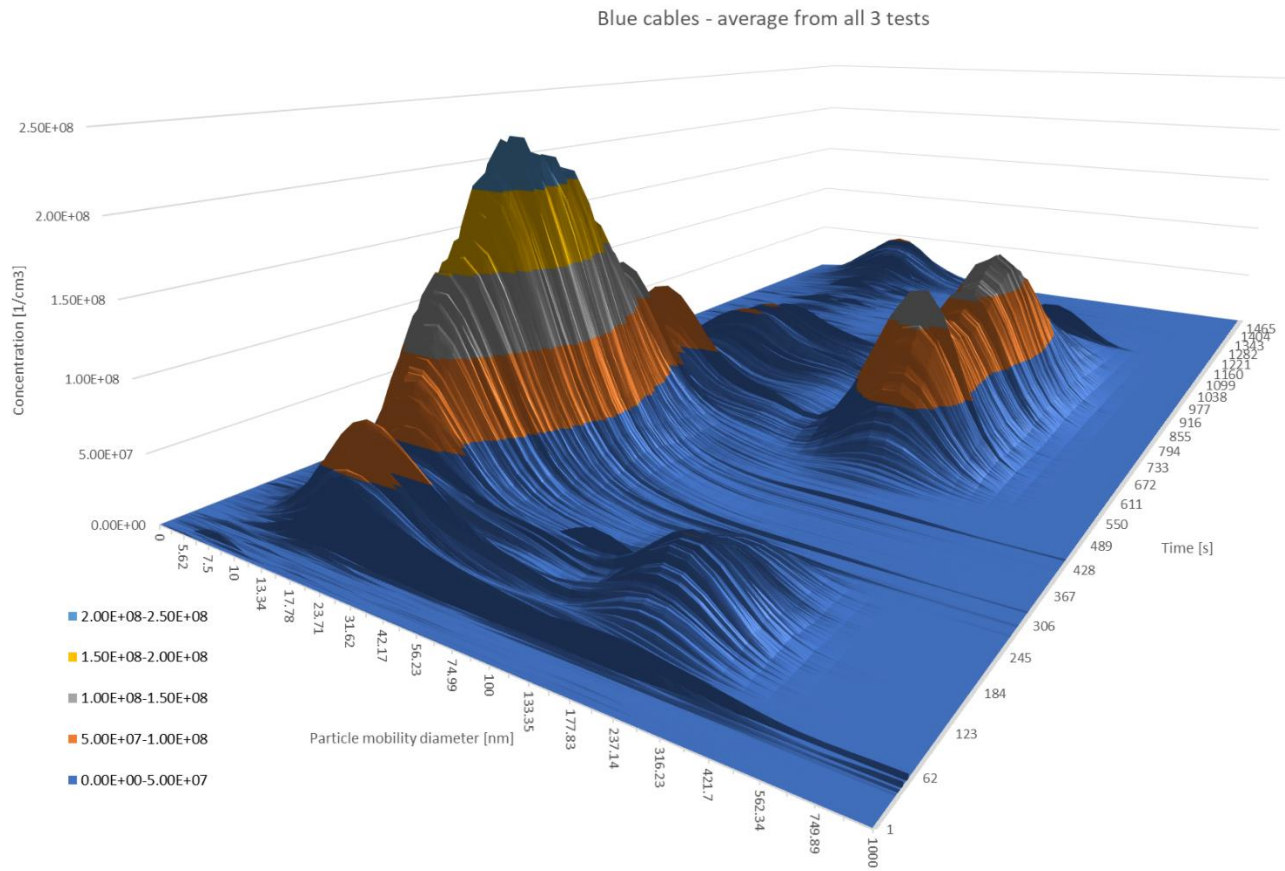


Figure 52 - Concentration vs Mobility Diameter vs Time - Blue Cables (C01) – average from all 3 tests

On the other hand, dominance of 2<sup>nd</sup> mode particles is clear in Shell Diala oil as it can be observed in figure 52.

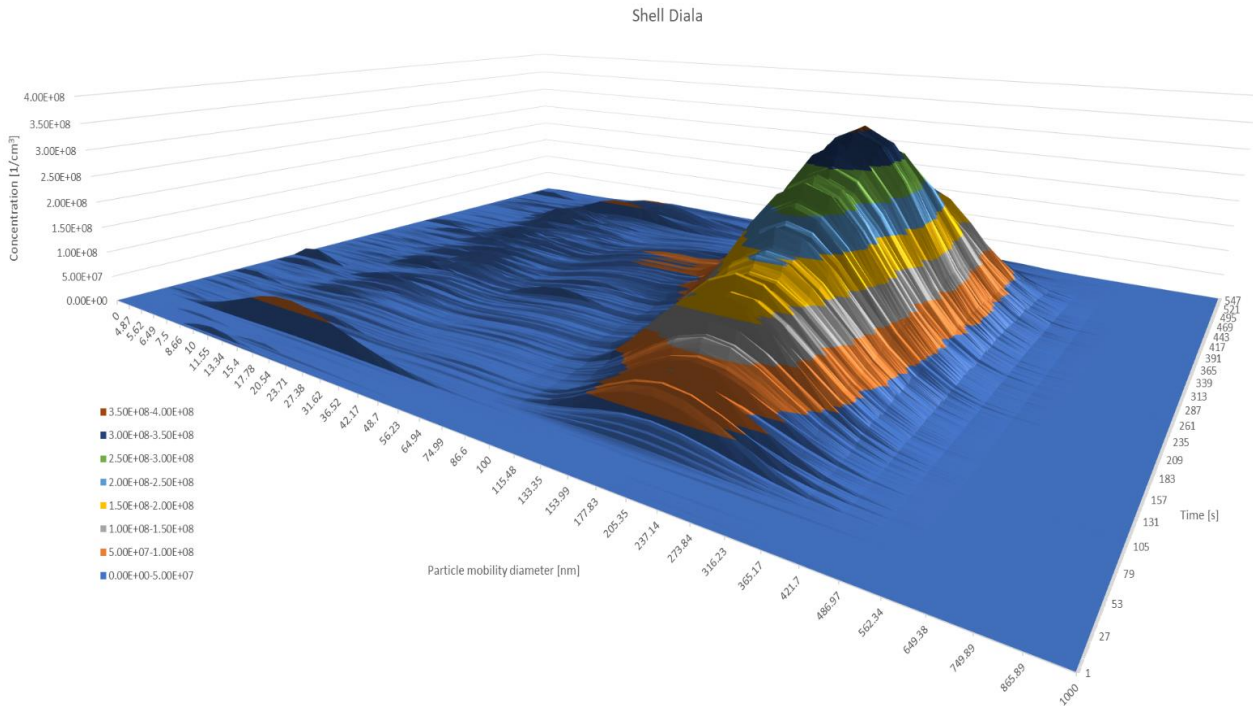


Figure 53 - Concentration vs Mobility Diameter vs Time - Shell Diala – average from all 3 tests

### 3.4 SUMMARY OF EXPERIMENTAL RESULTS

The following table summarizes major results from experiments:

*Table 6 - Summary of experimental results*

Exp. Description	mean(CMD_nucl)	std(CMD_nucl)	mean(CMD_acc)	std(CMD_acc)	mean(Conc_nucl)	std(Conc_nucl)	mean(Conc_acc)	std(Conc_acc)
Blue Cables #1	75.96	80.80	216.70	185.77	2.896E+07	3.536E+07	1.163E+07	1.605E+07
Blue Cables #2	28.59	38.89	171.97	77.95	3.327E+07	3.649E+07	1.508E+07	1.780E+07
Blue Cables #3	38.68	55.04	153.02	65.20	3.123E+07	3.409E+07	1.418E+07	1.582E+07
Black Cables #1	58.23	72.55	219.04	190.74	2.002E+07	2.904E+07	7.894E+06	1.063E+07
Black Cables #2	44.41	55.42	145.75	80.21	2.470E+07	3.253E+07	6.814E+06	9.547E+06
Black Cables #3	60.73	73.70	161.31	71.79	2.230E+07	3.019E+07	2.869E+06	3.889E+06
Brown Cables #1	44.16	55.22	173.36	39.71	3.236E+07	3.185E+07	1.891E+07	2.002E+07
Brown Cables #2	32.18	36.35	177.93	49.95	3.194E+07	2.778E+07	1.978E+07	2.050E+07
Brown Cables #3	37.78	60.98	160.07	78.11	2.917E+07	2.838E+07	1.452E+07	1.655E+07
Shell Diala #1	105.82	65.49	204.05	31.12	2.121E+07	1.809E+07	5.453E+07	4.087E+07
Shell Diala #2	77.81	36.07	201.06	44.33	2.886E+07	2.959E+07	6.849E+07	8.470E+07
Shell Diala #3	78.03	49.66	218.23	43.94	2.283E+07	1.947E+07	5.705E+07	4.445E+07
Midel #1	62.17	40.27	190.62	50.59	1.632E+07	2.218E+07	2.511E+07	2.107E+07
Midel #2	85.83	70.64	200.79	51.49	1.603E+07	2.449E+07	2.382E+07	2.058E+07
Midel #3	83.04	73.04	208.96	46.68	1.659E+07	3.408E+07	2.111E+07	2.139E+07

CMD = Count Mean Diameter [nm]      STD = Standard Deviation      nucl = nucleation (1st) mode      acc = accumulation (2nd) mode

It can be observed that in general results vary greatly (e.g. mean CMD in nucleation mode for blue cables varies from 28 to 76 nm). The dominance of 1<sup>st</sup> mode (nucleation) particles concentration in cables is easily visible from the table. The same stands for dominance of 2<sup>nd</sup> mode (accumulation) particles for oils, particularly visible in Shell Diala oil. It is also shown that count mean diameter (CMD) in nucleation mode (1<sup>st</sup> mode) shown on average smaller values for cables then for oils. Same stands for CMD in accumulation, where average particle diameter was slightly bigger in oils then in cable tests. Certainly, more repetitions of experiments would result in more precise results and more conclusions could be drawn. Nevertheless, these results still show some trends and typical behaviours of the samples tested, and look promising, thus they could be only improved with further testing.

## 4 CONCLUSIONS AND FUTURE WORK

---

### 4.1 CONCLUSIONS

In the first part of this thesis, an Excel calculator giving design fire for electrical cabinets and racks present in CERN is developed. Findings from experiments conducted in the USA, Finland and France were used to obtain an envelope case covering the worst possible case. The user can specify any combination between the most basic one – a single cabinet, to the most severe one – 2 rows containing 10 cabinets each. On top of that, the user can specify positions of each cabinet defining if it is a closed cabinet or an open cabinet (or a rack), which further affects the values for heat release rate and the duration of the fire. If no data on fuel content present in cabinets is known, worst case values obtained in experiments of 500kW for closed and 1000kW for open cabinets are used. On the other hand, if combustible contents are known, the user can specify their weight, which will still affect the duration of steady burning, but the peak HRR values will remain the same as the chosen values were highest possible values expected in a cabinet. Finally, the prescribed value of 500kW for closed cabinets is validated by calculating it according to three separate models developed in France and Finland, and it was confirmed that the chosen value was reasonable.

In the second part, an attempt to address the fire severity of vehicles used in CERN is made. Most of the literature related to vehicle fires deals with fires in passenger cars and buses and in mining vehicles, that are all way bigger and heavier than the small electrical tractors used in CERN, and thus have way higher HRRs. Because of this, it was difficult extrapolating and making conclusions about CERN vehicles. Nevertheless, an experimental campaign on electrical forklifts was conducted at IRSN in France, and HRR curve for a typical forklift is suggested to be used for CERN electrical tractors, as it resembles them largely. Another methodology for assessing HRR in vehicles is proposed, which requires knowledge of HRR of each individual component of the vehicle. HRR values for bus seats and mining vehicle tyres are given and could be useful when using this methodology.

In the third part, an experimental campaign is conducted on three types of most common cables used in CERN, as well as on two most common insulating oils used in CERN. The goal of the experiments was to obtain detailed smoke characterization of the specimens, which would be extremely useful for validating and further developing FDS modelling related to aerosol deposition and particle distribution. CERN is in particular interested in these results, as smoke particles are expected to carry radiation further away from the seat of the fire, which is a great hazard both for the facility and for environment. A bimodal distribution in particle size was observed especially in cable tests where 1<sup>st</sup> mode ( $d_m < 100\text{nm}$ ) particles were dominant in the first part of burning (burning of outer sheath), while 2<sup>nd</sup> mode particles ( $100 \text{ nm} < d_m < 1000\text{nm}$ ) were dominant in the second part of burning (burning of the sheath of wires), meaning that they were made of different materials. Several materials showed unexpected and unclear behaviour. For example, Midel oil showed extreme peaks in concentration both at the very beginning and at very end of tests, and this behaviour was repeated in all 3 tests.

Black cables showed really high peaks in concentration only at very beginning of burning. No general conclusions could be made when comparing HRR and concentration values for cables, as they showed quite unpredictable trends. Overall, oils showed great accordance both in HRR and in concentration values in all tests, which is expected as they are more homogenous and thus burn more steadily than cables.

An estimation of mass concentration was made according to the density correction factor developed for diesel engine exhaust, as no further knowledge was obtained about density of cable and oil particles.

## 4.2 FUTURE WORK

Excel calculator developed for electrical cabinets and racks can if needed be extended to more cabinets. On top of that, if other fuel types than cabinets and racks can be present at some positions, they could be included in the calculator. Also, as only one cabinet experimental session was conducted by now in “confined enclosure” conditions, and it was done only for closed cabinets, it would be interesting doing more experiments in smaller confined compartments, especially for seeing the impact of heat accumulated in confined hot smoke layer on the fire growth and spread in cabinets, both for closed and for open cabinets. In addition to that, it would be interesting seeing if the fire would spread from one row of cabinets to another positioned at a certain distance (e.g. 1 m away).

For vehicle fires, main issue that has to be addressed in future are fires in batteries, and how they affect the overall heat released during vehicle fire. Also, as there is almost no literature on fires in small vehicles, an experimental campaign on full scale vehicles used in CERN, or at least on individual components would be extremely useful, and would allow more precise description of fire behaviour of each individual vehicle used in CERN.

To author's knowledge, the tests conducted with DMS500 coupled with cone calorimeter, were a first attempt of a kind in characterizing particle size distribution in cables and oils. Results obtained are more than promising. In order to further validate them more repetitions should be performed. It is advised to use a camera to record all experiments, as it would additionally help in explaining the phenomena observed.

## 5 ACKNOWLEDGMENTS

---

First of all, I would like to thank my supervisor professor Patrick Van Hees, for providing support and helping whenever needed throughout the whole semester. Furthermore, professor Van Hees and Dan Madsen made it possible to obtain and use the fast particle analyser DMS500, which was crucial for the completion of this thesis and added a great value to this work.

Not less important was my co-supervisor from CERN, Oriol Rios Rubiras, who gave very interesting and useful suggestions throughout the whole thesis time. It was more than pleasant having an IMFSE alumnus as a co-supervisor, and I am more than happy that Oriol remained involved in IMFSE, at least through supervising, as it is a great mutual benefit for IMFSE, for Oriol and for students that are supervised by him.

Thanks to another supervisor of my thesis - Saverio La Mendola from CERN, for keeping up with my work for the whole time, and for giving valuable advice and a lot of encouraging words. It meant a lot.

Many thanks to Dan Madsen for helping me organize the experiments, and for promptly replying to all inquiries I had. Your help made this thesis a lot easier for me.

Thanks to Louise Gren from aerosol division for helping in setting up DMS500 and later analysing the output. Some key uncertainties were eliminated thanks to your advice.

Thank you, Stefan Svensson, for assisting and helping successfully finish the lab experiments.

A great thanks to my good friend from bachelor studies, and luckily my IMFSE colleague nowadays, Balša Jovanović. Your knowledge, your patience and your willingness to help at any time will always be remembered.

Another key person that helped me finish this thesis was my brother Boris. Your encouragement and support have pushed me through my whole education process, from elementary school until today. Your expertise in programming and help in solving the MATLAB bugs that bothered me were priceless.

My mother Branka and my father Vladimir, the two kindest persons I know, have inspired, encouraged, and with their wise words advised me for 26 years and counting. My eternal gratitude goes to you.

Finally, I would like to thank the whole IMFSE team for creating this unique and incredible program, and for giving me the honour of being a part of it. I consider my time spent in IMFSE as the most flourishing two years of my life, because of academic benefits I gained, but even more because of all the wonderful people I met on this journey.

## 6 REFERENCES

---

- [1] Hurley, M. J., *Performance-Based Fire Safety Design*. .
- [2] Isaksson, E. and Olin, F., "Comparative study of risk analysis methods from a fire safety perspective," LUND UNIVERSITY, 2016.
- [3] Chavez, J. M., "Experimental Investigation of Internally Ignited Fires in Nuclear , Power Plant Control Cabinets : Part 1 : Cabinet Effects Tests," no. April, 1987.
- [4] Mangs, J. and Keski-Rahkonen, O., *Full scale fire experiments on electronic cabinets I*. 1994.
- [5] Mangs, J. and Keski-Rahkonen, O., *Full scale fire experiments on electronic cabinets II*. 1996.
- [6] Mangs, J., "On the fire dynamics of vehicles and electrical equipment," *VTT Publ.*, no. 521, pp. 3–62, 2004.
- [7] Mangs, J., Paananen, J., and Keski-Rahkonen, O., "Calorimetric fire experiments on electronic cabinets," *Fire Saf. J.*, vol. 38, no. 2, pp. 165–186, 2003.
- [8] Plumecocq, W., Coutin, M., Melis, S., and Rigollet, L., "Characterization of closed-doors electrical cabinet fires in compartments," *Fire Saf. J.*, vol. 46, no. 5, pp. 243–253, 2011.
- [9] Coutin, M., Plumecocq, W., Zavaleta, P., and Audouin, L., "Characterisation of open-door electrical cabinet fires in compartments," *Nucl. Eng. Des.*, vol. 286, pp. 104–115, 2015.
- [10] Melis, S., Rigollet, L., Such, J. M., and Casselman, C., "Modelling of Electrical Cabinet Fires based on the CARMELA Experimental Program."
- [11] Kassawara, R. P. and Hyslop, J. S., "EPRI / NRC-RES Fire PRA Methodology for Nuclear Power Facilities (EPRI-1011989 and NUREG/CR-6850) Volume 2 : Detailed Methodology," vol. 2, 2005.
- [12] Zahirasri, M., Tohir, M., and Spearpoint, M., "Distribution analysis of the fire severity characteristics of single passenger road vehicles using heat release rate data," *Fire Sci. Rev.*, 2013.
- [13] Hansen, R., "Design fires in underground hard rock mines," *Thesis*, no. 127, 2011.
- [14] Conference, I., "Battery Aspects on Fires in Electrified Vehicles," p. 274, 2016.
- [15] Sturk, D., Hoffmann, L., and Ahlberg Tidblad, A., "Fire Tests on E-vehicle Battery Cells and Packs," *Traffic Inj. Prev.*, vol. 16, pp. 159–164, 2015.
- [16] Larsson, F., Andersson, P., and Mellander, B.-E., "Lithium-Ion Battery Aspects on Fires in Electrified Vehicles on the Basis of Experimental Abuse Tests," *Batteries*, vol. 2, no. 2, p. 9, 2016.

- [17] Composites, L., "Experimental Characterization of a forklift fire," vol. 36, no. 13, pp. 3–5, 2002.
- [18] Fontaine, G., Ngohang, F. E., Gay, L., and Bourbigot, S., "Investigation of the Contribution to Fire of Electrical Cable by a Revisited Mass Loss Cone," *Fire Sci. Technol.*, pp. 687–693, 2015.
- [19] Klippel, N., Nussbaumer, T., and Hess, A., *Particle Emissions from Residential Wood Combustion – Design and Operation Conditions*. 2005.
- [20] Helsper, C., Fissan, H. J., Muggli, J., and Scheidweiler, A., "Particle number distributions of aerosols from test fires," *J. Aerosol Sci.*, vol. 11, no. 5–6, pp. 439–446, 1980.
- [21] Wang, F. *et al.*, "Ignition of Energized PVC-Insulated Electrical Wires and Characteristics of Smoke Particles Formed during Combustion," pp. 374–382.
- [22] Slowik, J. G. *et al.*, "Particle morphology and density characterization by combined mobility and aerodynamic diameter measurements. Part 2: Application to combustion-generated soot aerosols as a function of fuel equivalence ratio," *Aerosol Sci. Technol.*, vol. 38, no. 12, pp. 1206–1222, 2004.
- [23] Butler, K. M. and Mulholland, G. W., "Generation and Transport of Smoke," *Fire Technol.*, pp. 149–176, 2004.
- [24] Babrauskas, V. and Peacock, R. D. ., "Hear Release Rate: The Simple Most Important Variable in Fire Hazard," *Fire Saf. J.*, vol. 18, pp. 255–272, 1991.
- [25] Makhviladze, G. M., *Enclosure fire dynamics*, vol. 37, no. 1. 2002.
- [26] ISO/TR, B. S. B., "Fire safety engineering - Part 2 : Design fire scenarios and design fires," 1999.
- [27] Hansen, R., "Methodologies for calculating the overall heat release rate of a vehicle in an underground structure .," *Mälardalen Univ.*
- [28] Ingason, H., "Fire test with a front wheel loader rubber tyre," 2010.
- [29] Overholt, K. J., Floyd, J. E., and Ezekoye, O. A., "Computational Modeling and Validation of Aerosol Deposition in Ventilation Ducts," *Fire Technol.*, vol. 52, no. 1, pp. 149–166, 2016.
- [30] Gottuk, D., Mealy, C., and Floyd, J., "Smoke transport and FDS validation," *Fire Saf. Sci.*, pp. 129–140, 2008.
- [31] British Standards Institution, "BS ISO 5660-1:2015. Reaction-to-fire tests — Heat release , smoke production and mass loss rate. Part 1 : Heat release rate (cone calorimeter method) and smoke production rate (dynamic measurement)," p. 66pp, 2015.
- [32] Cambustion Ltd., "DMS500 MkII The Rapid Response Engine Particulate Analyzer."
- [33] BSI, "Fire hazard testing — part 8.3. Heat Release of insulating liquids used in

electrotechnical products," *October*, vol. 3, no. 1, 2003.

- [34] TSI, I., "Aerosol Statistics, Lognormal Distributions, and dN / dlogDp," pp. 1–6, 2012.
- [35] Analyzer, F. P., "Fast Particulate Analyzer - user manual," pp. 1–140, 2015.
- [36] Park, K., Cao, F., Kittelson, D. B., and McMurry, P. H., "Relationship between particle mass and mobility for diesel exhaust particles," *Environ. Sci. Technol.*, vol. 37, no. 3, pp. 577–583, 2003.
- [37] IEC, "Reaction-to-fire tests — Heat release, smoke production and mass loss rate," *IEC 60721-3-3, Classif. Environ. Cond. Part 3-3 Classif. groups Environ. parameters their Sev. Station. use Weather. Locat.*, vol. 2002, no. part 2-Smoke production rate (dynamic measurement), 2002.

## 7 APPENDICES

### 7.1 APPENDIX A – CONCENTRATION GRAPHS

Table 7- Concentration graphs - Midel oil

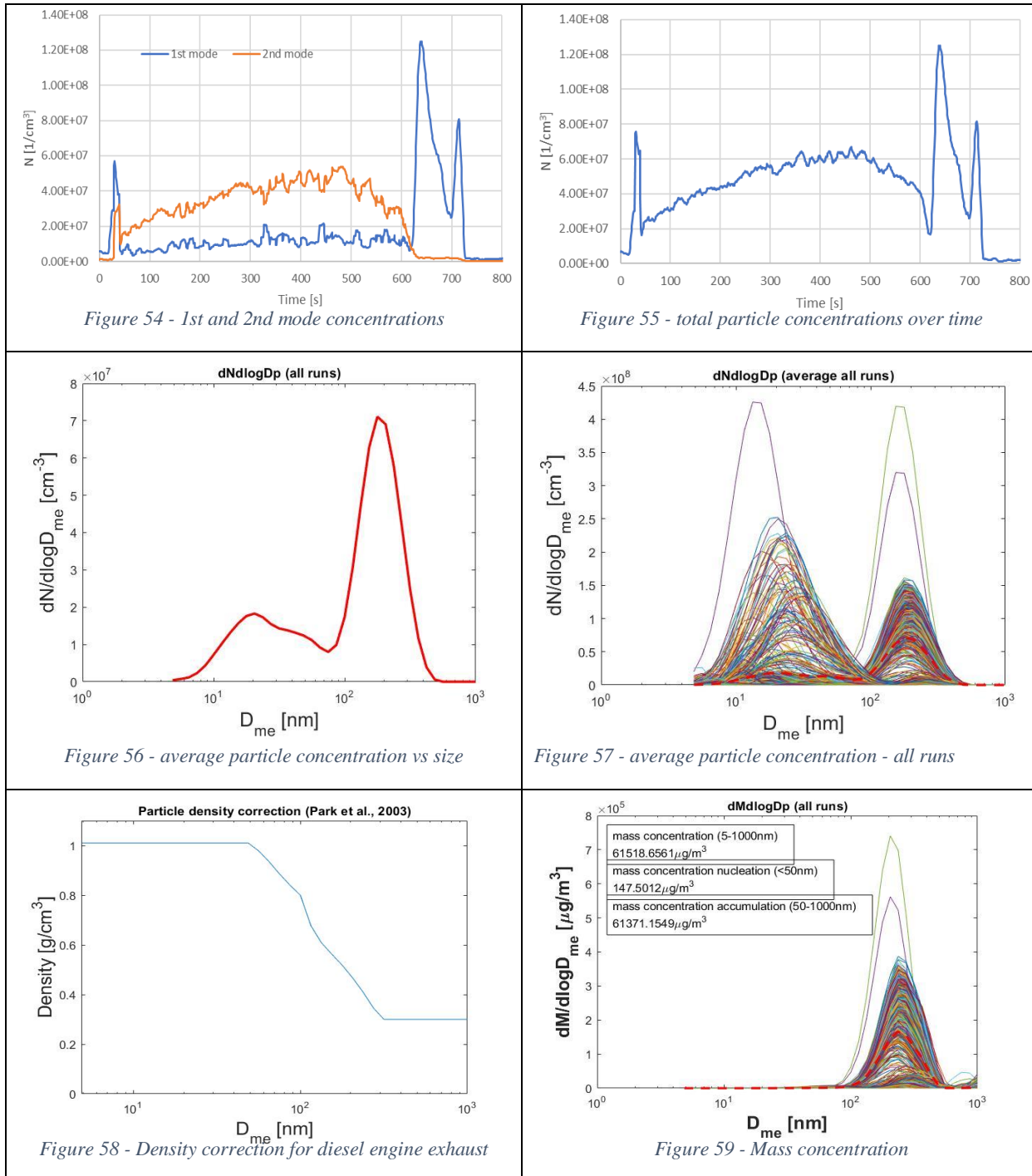


Table 8 - Concentration graphs - Black cables

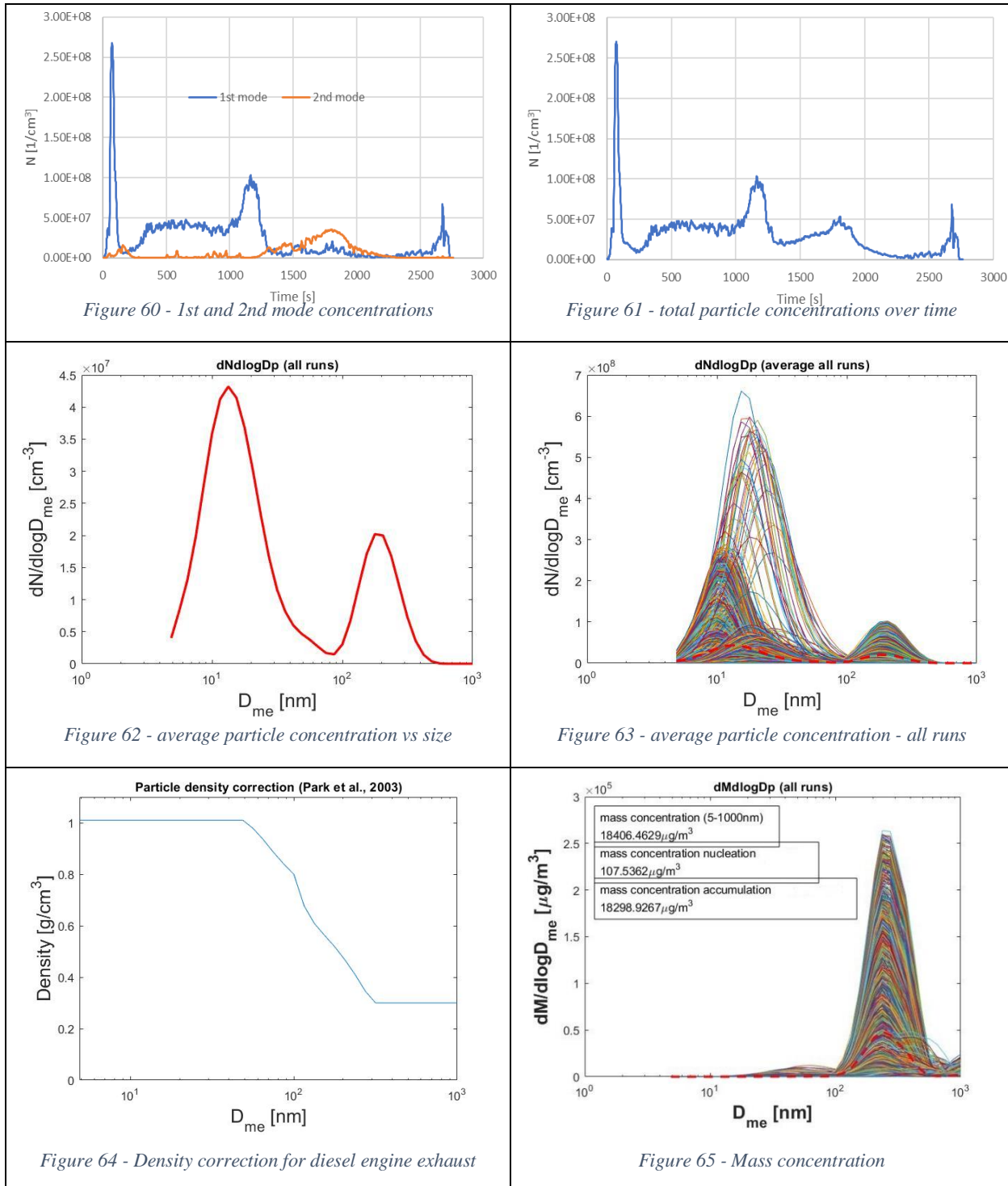
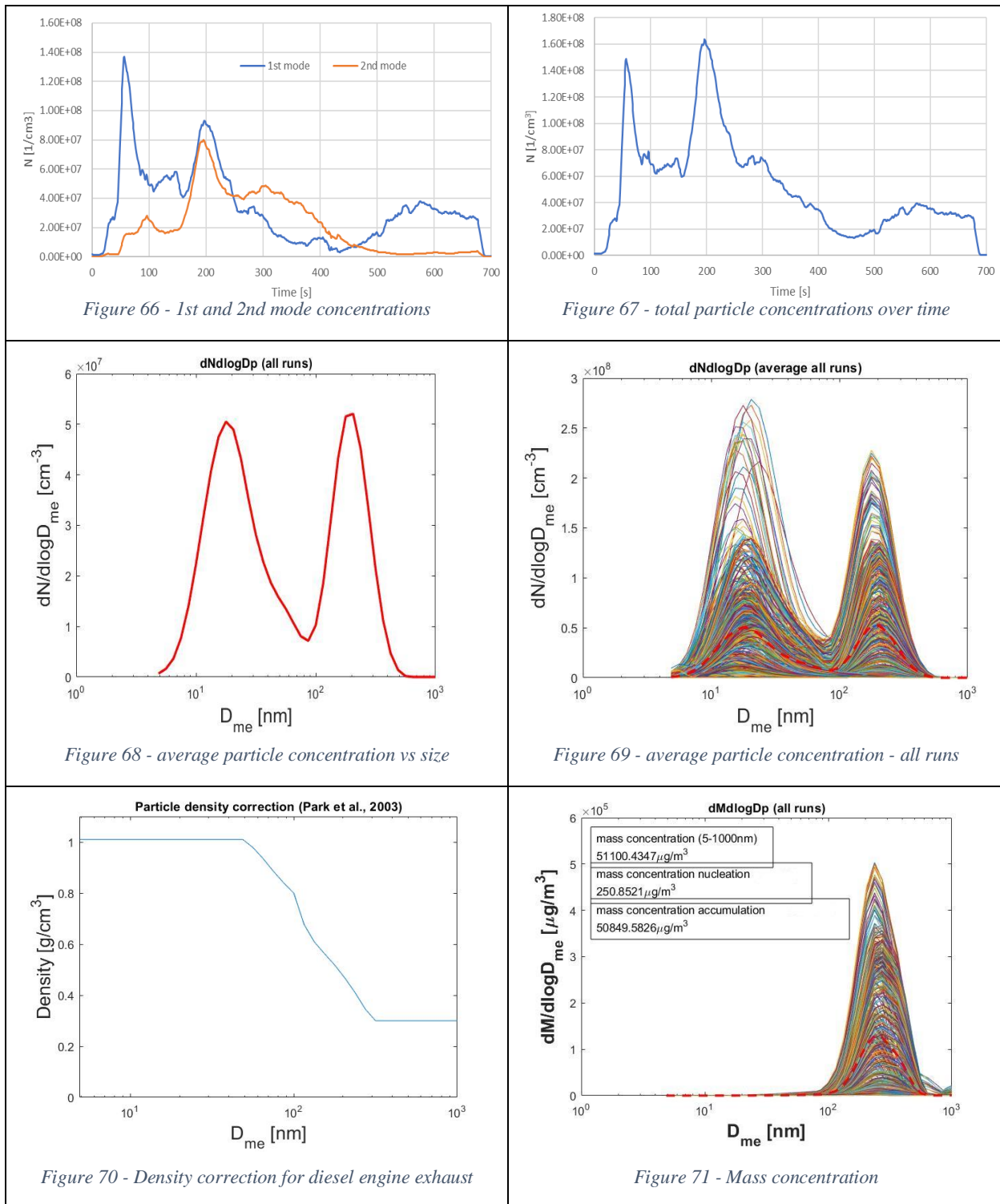
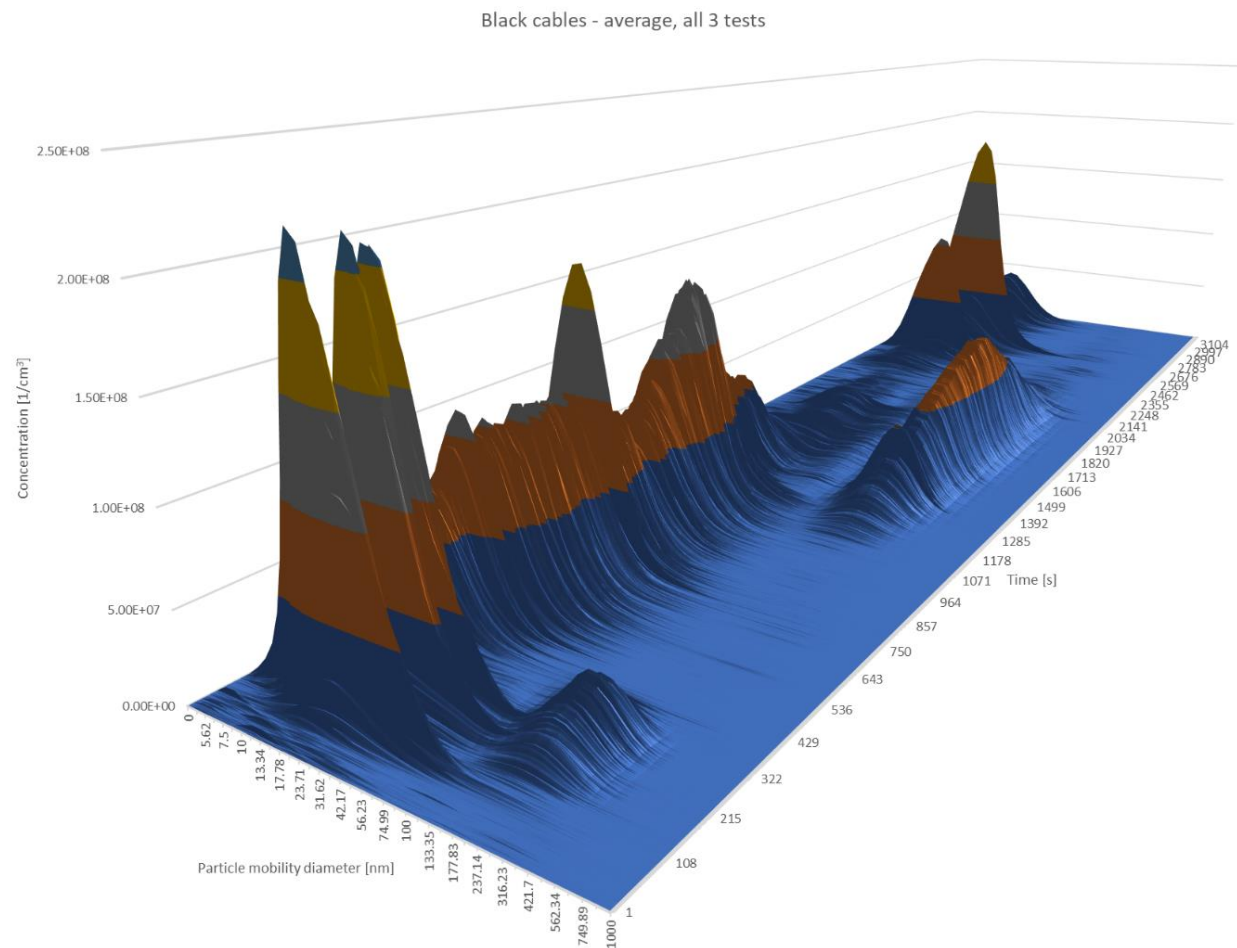


Table 9 - Concentration graphs – brown cables



## 7.2 APPENDIX B – 3D PLOTS



*Figure 72 - Concentration vs Mobility Diameter vs Time – black cables – average from all 3 tests*

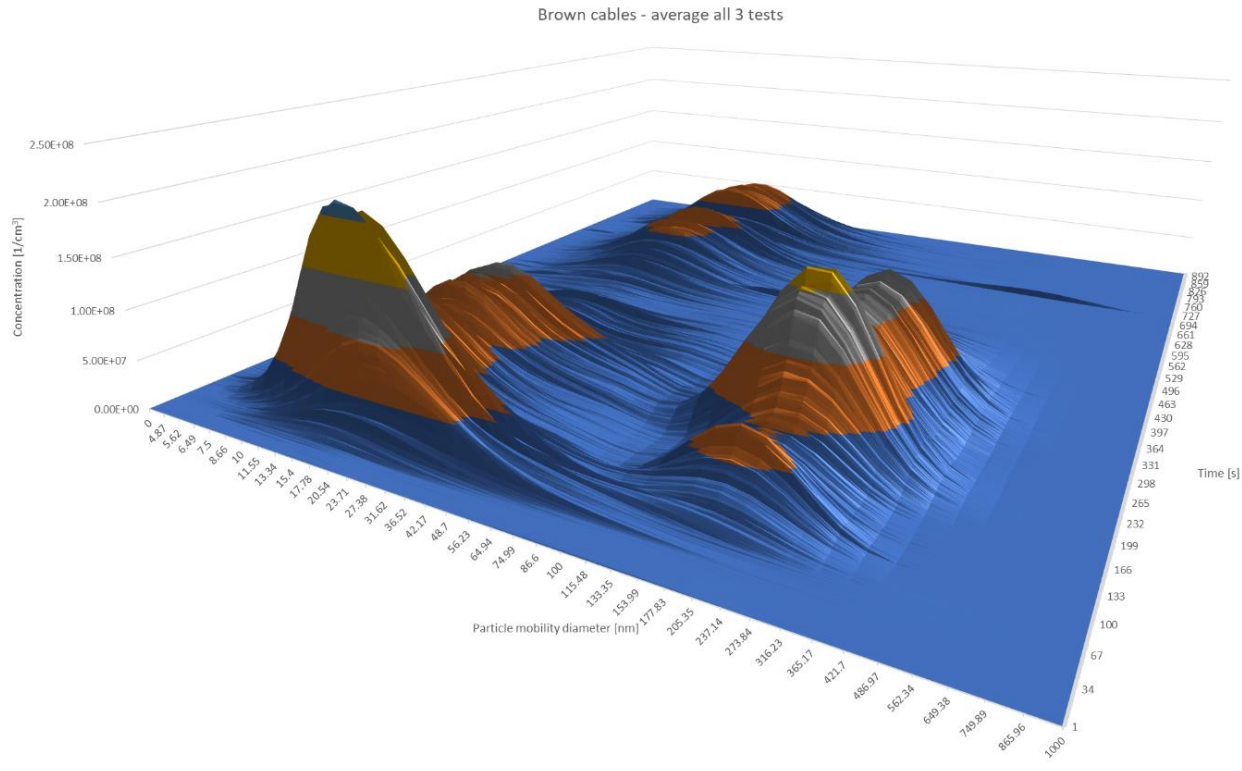


Figure 73 - Concentration vs Mobility Diameter vs Time – brown cables – average from all 3 tests

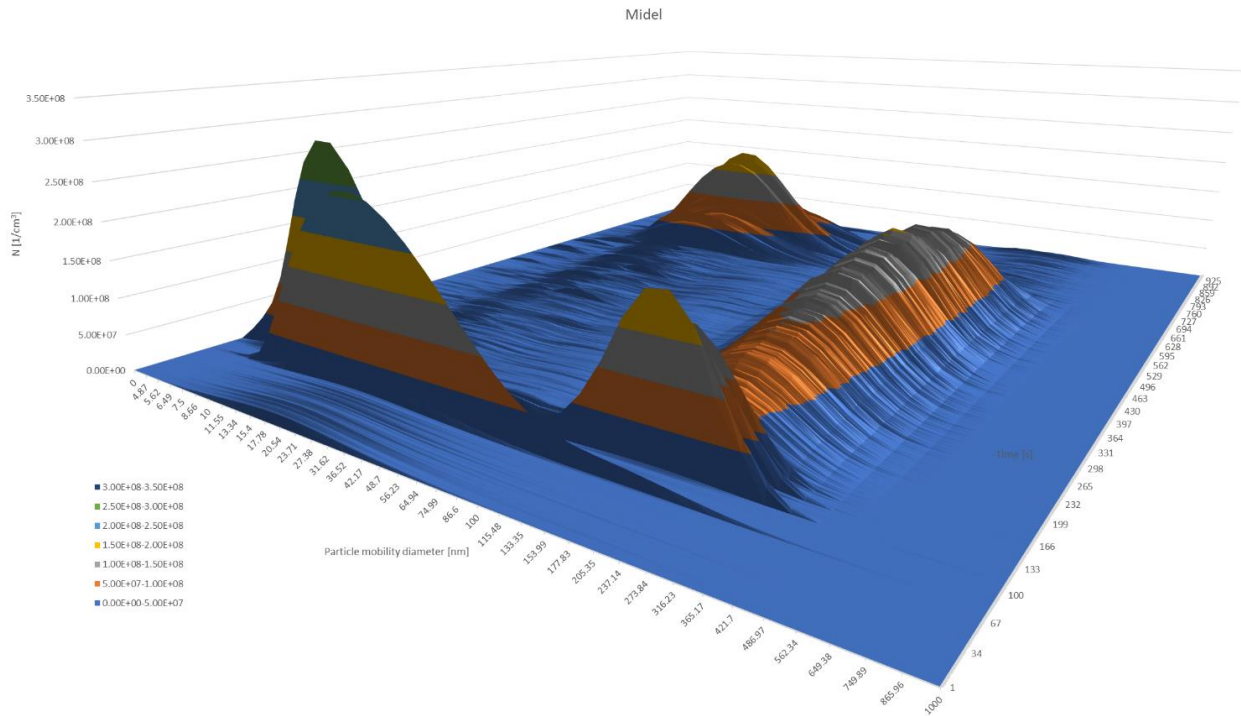


Figure 74 - Concentration vs Mobility Diameter vs Time – Midel oil – average from all 3 tests

### 7.3 APPENDIX C – CO AND CO2 YIELDS

Averages of CO and CO2 yields for all the specimens are given in the following table:

*Table 10 - CO and CO2 yields - all specimens*

Yields	Blue Cables C01	Black Cables C02	Brown Cables C04	Shell Diala	Midel
CO yield [kg/kg]	0.025-0.086	0.012-0.019	0.022-0.025	0.022	0.0145
CO2 yield [kg/kg]	1.14-5.28	0.73-1.1	1.4-1.5	2.67	2.27

Both oils, shown more steady values, thus only average values are given for their CO and CO2 yields. On the other hand, cables showed a lot of fluctuation – especially blue cables, varying in CO yield from 0.025 to 0.086 kg/kg fuel burnt. Even with a lot of smoothening, graphs for CO and CO2 yields showed quite odd behavior and a lot of extreme peaks, thus they will not be shown. Still, for the sake of completion, they will be provided to CERN in the raw .csv form. Nevertheless, values given in table can be used as good guidelines, and could be useful in FDS modelling, apart from Blue Cables results that certainly require more analysis (testing).

## 7.4 APPENDIX D – TOTAL CONCENTRATION GRAPHS- ALL 3 TESTS

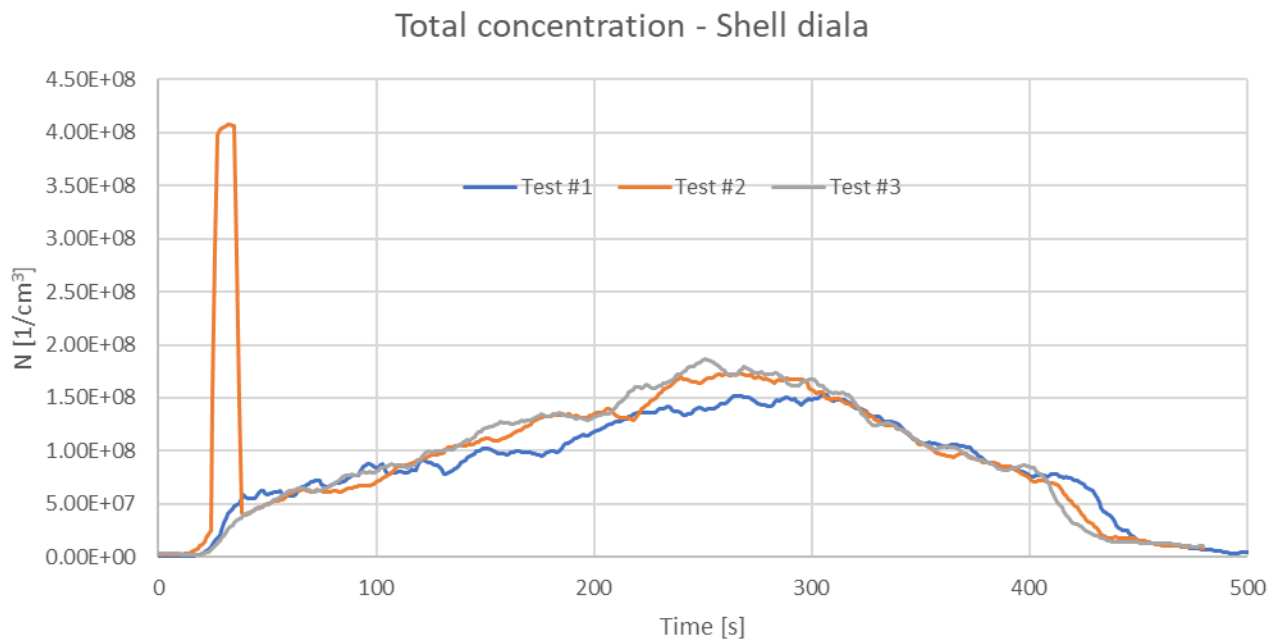


Figure 75 - Total concentration - All 3 tests -Shell Diala

A peak observed at the start of burning of Test #2 is believed to have been noise. Unfortunately, no videos are available to check if anything unusual in burning behavior occurred at that time.

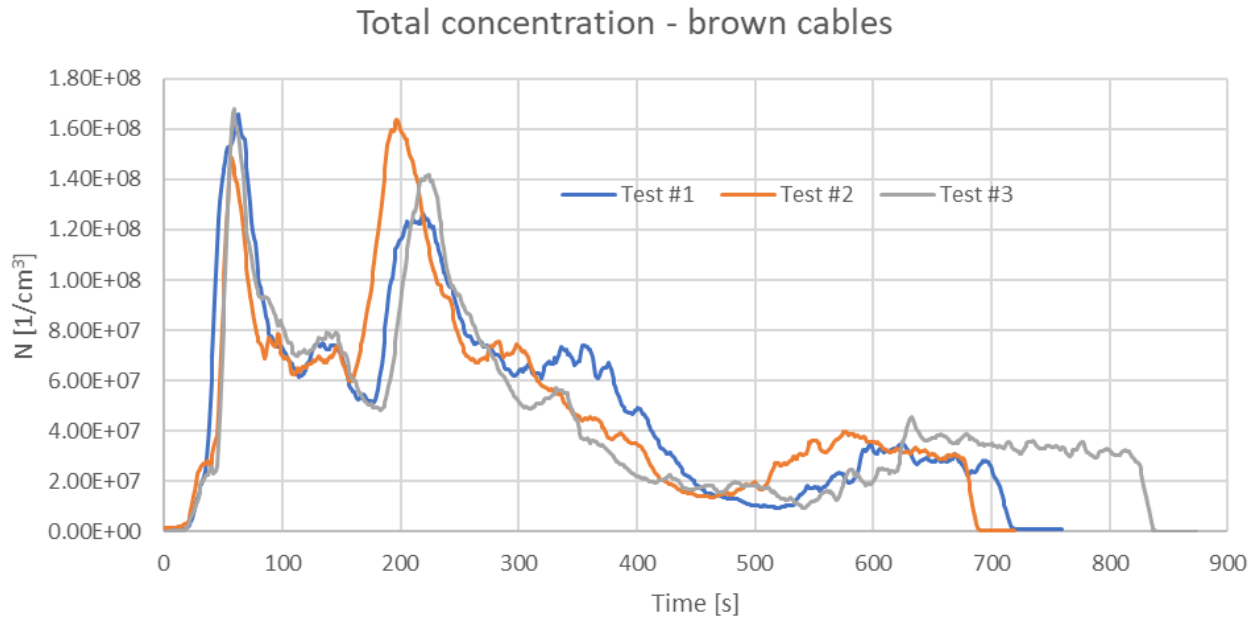


Figure 76 - Total concentration - All 3 tests - Brown cables (C04)

## 7.5 APPENDIX E – HRR GRAPHS – ALL 3 TESTS

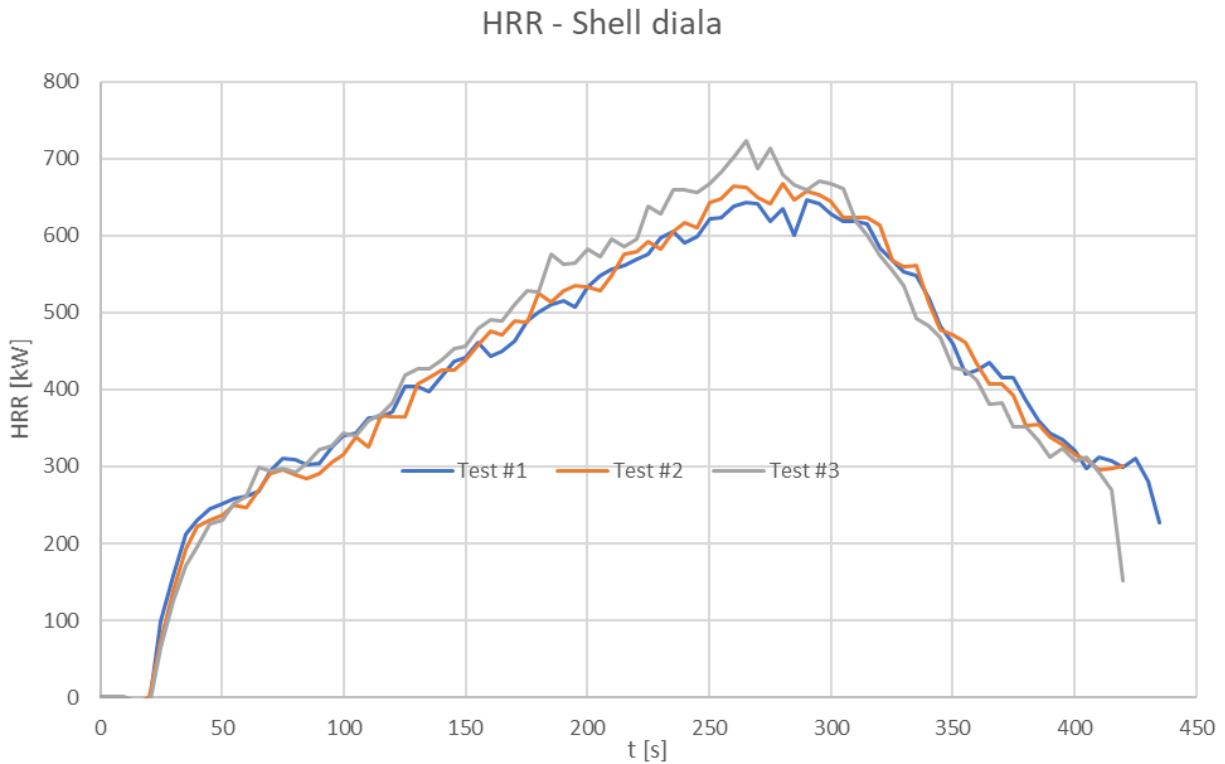


Figure 77 - HRR graphs - all 3 tests - Shell Diala oil

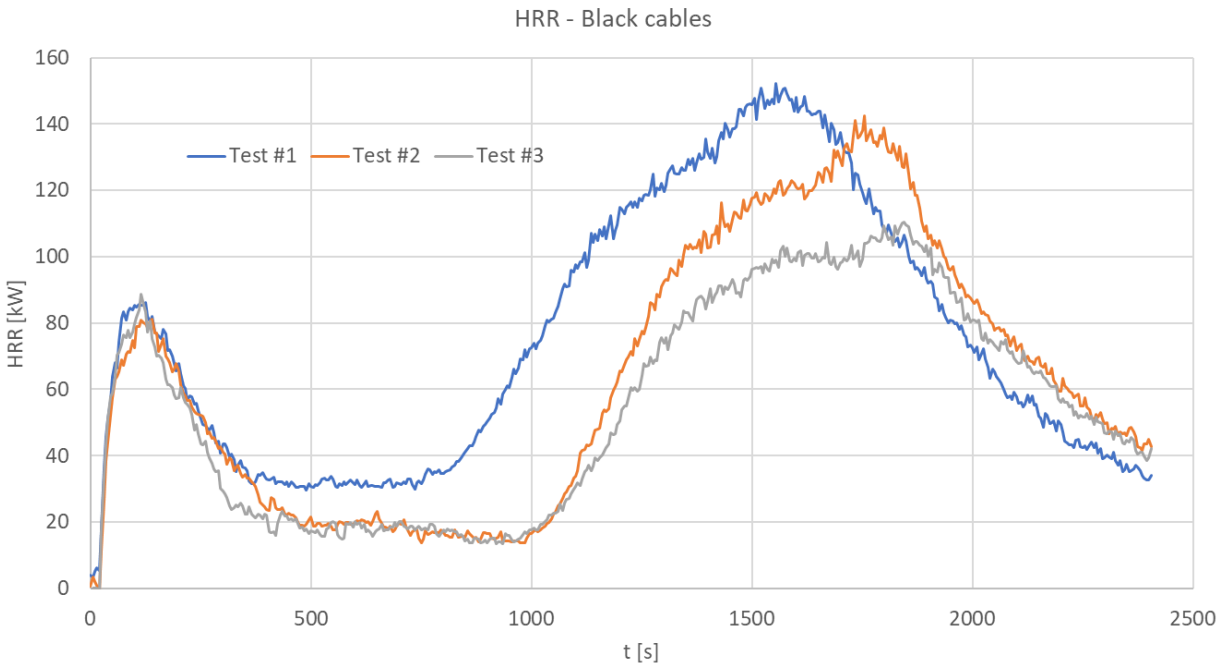


Figure 78 - HRR graphs - all 3 tests - Black Cables C02

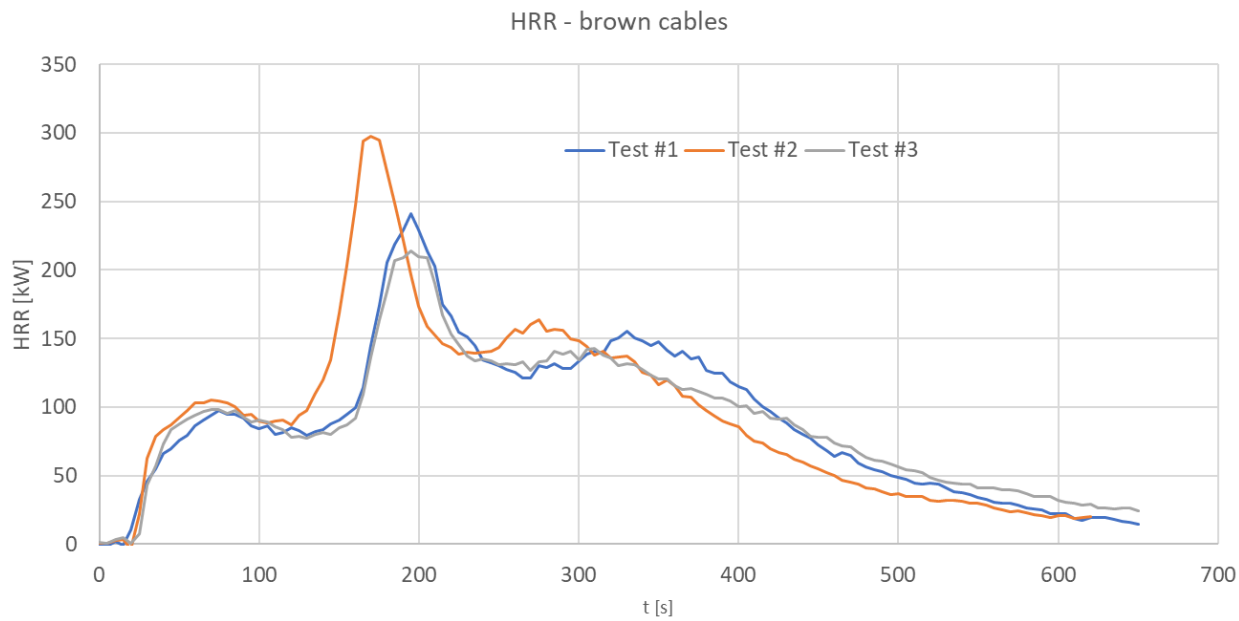


Figure 79 - HRR graphs - all 3 tests - Brown Cables C04

## 7.6 APPENDIX F – SMOKE PRODUCTION RATE VS CONCENTRATIONS - CABLES

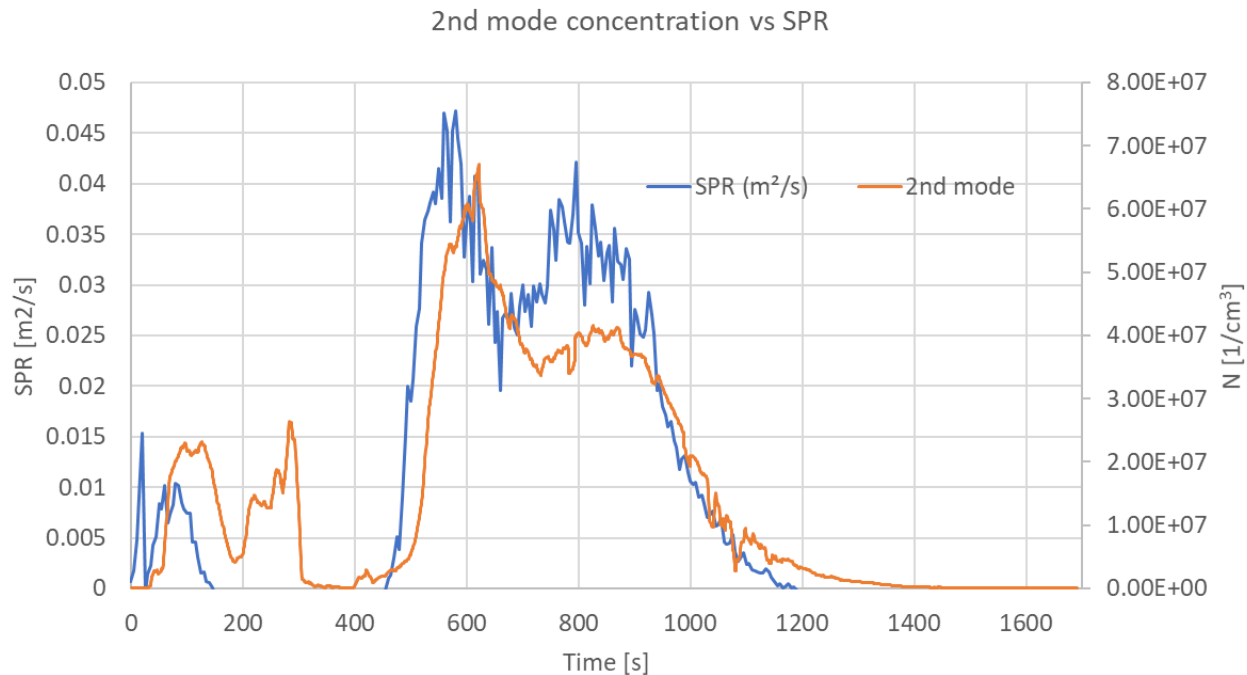


Figure 80 - 2nd mode conc. vs SPR - Blue Cables (C01)

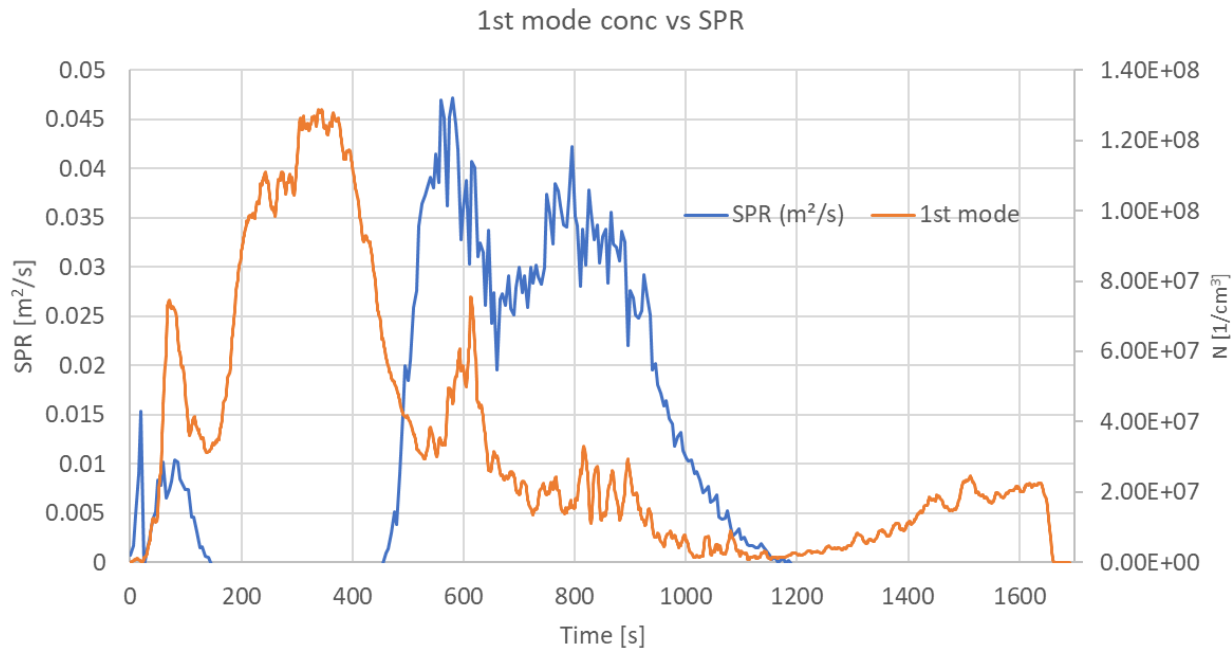


Figure 81 - 1st mode conc vs SPR - Blue Cables (C01)

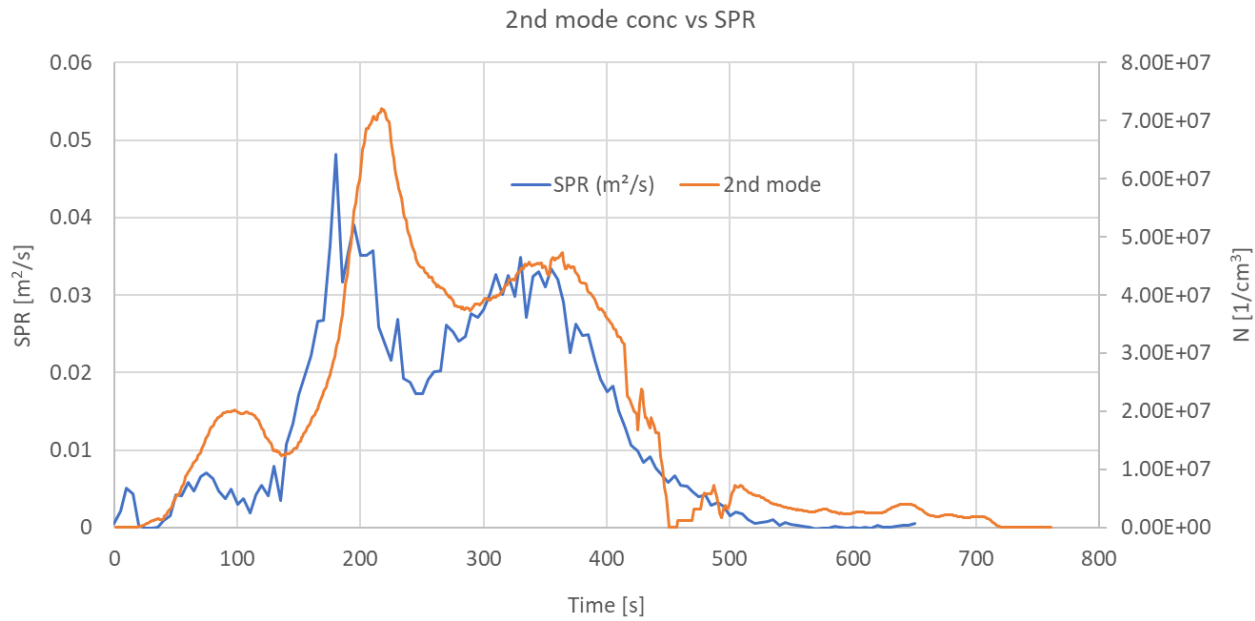


Figure 82 - 2nd mode conc vs SPR - Brown cables (C04)

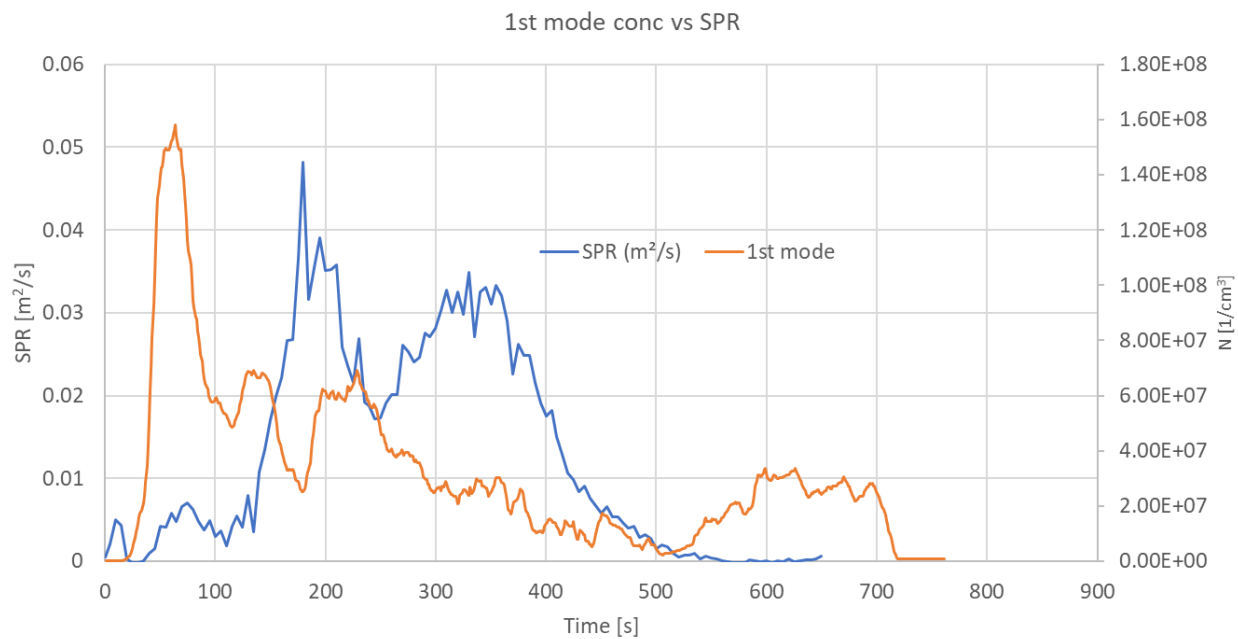


Figure 83 - 1st mode conc vs SPR - Brown Cables (C04)

## 7.7 APPENDIX G – EXCEL CALCULATOR EXPLANATION

Figure 7 shows the main sheet from the Excel calculator used to obtain design fires in electrical cabinets/racks present in CERN. User is at first required to specify the total number of rows and columns of cabinets (e.g. 2 rows 6 columns, so 12 cabinets in total like in the example shown). After that, a green box appears representing the total number of cabinets – 12 in this case. User is then required to fill each of the green cells with either number 0 – representing an open cabinet (or a rack), or with number 1 – representing a closed cabinet. Any distribution of open and closed cabinets is allowed. If the amount of combustibles inside of the cabinet is not known, user should fill the “amount of fuel” cell with 0. In this case, “combustible fraction” will not affect the result. In case the amount of combustibles inside the cabinet is known, user is required to specify it by filling the value in “amount of fuel” and in the “combustible fraction  $\chi$ ”. Finally, a graph showing the total HRR appears, designed according to explanations given in previous section. Major assumptions and notes are also mentioned in the box in the lower left corner of the main sheet, as it can be seen in figure 7.

On top of that, area of the HRR curve is integrated, giving the total amount of energy realised during the burning. The obtained value is then divided by the constant value of heat of combustion of 24 MJ/kg, giving the total expected amount of fuel (contents) inside of the cabinets corresponding to this size of a fire. It is shown in the yellow cell.

The full version of the Excel calculator file will be submitted in the CD form.

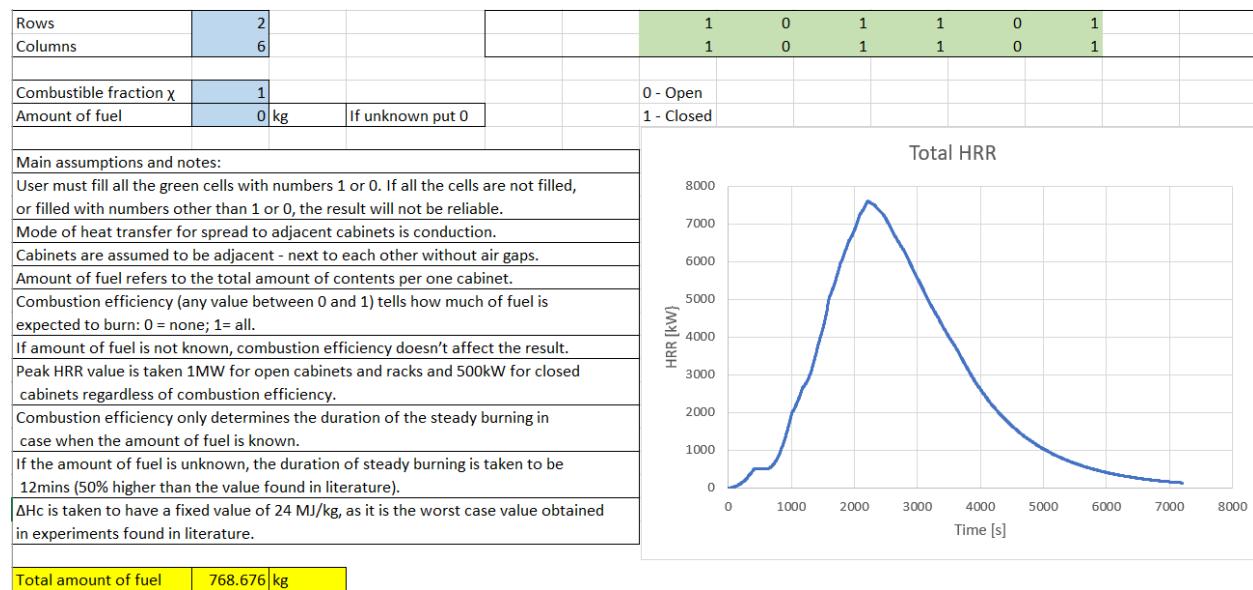


Figure 84 - Excel calculator for electrical cabinets - main input/output sheet